NOAA Atlas NESDIS 80
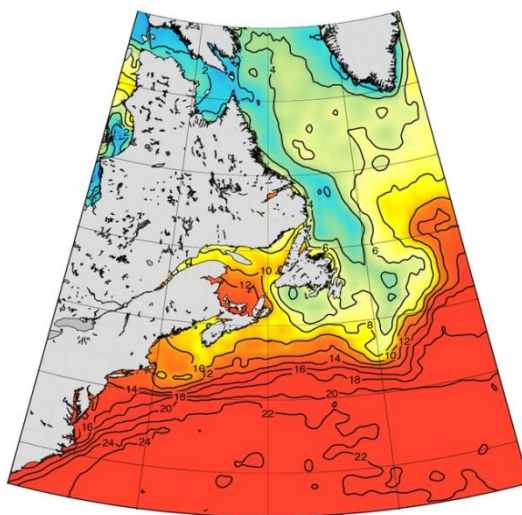
NORTHWEST ATLANTIC REGIONAL OCEAN CLIMATOLOGY

National Centers for Environmental Information
Silver Spring, Maryland

October 4, 2016

U.S. DEPARTMENT OF COMMERCE
National Oceanic and Atmospheric Administration
National Environmental Satellite, Data, and Information Service

National Centers for Environmental Information

Additional copies of this publication, as well as information about NCEI data holdings and services, are available upon request directly from NCEI.

National Centers for Environmental Information
User Services Team
NOAA/NESDIS
SSMC III, 4th floor
1315 East-West Highway
Silver Spring, MD 20910-3282

Telephone: (301) 713-3277
E-mail: NCEI.info@noaa.gov
NCEI URL: https://www.ncei.noaa.gov/

NOAA Atlas NESDIS 80

NORTHWEST ATLANTIC REGIONAL OCEAN CLIMATOLOGY

Seidov, D., O.K. Baranova, T. Boyer, S.L. Cross, A.V. Mishonov, and A.R. Parsons

National Centers for Environmental Information
Silver Spring, Maryland
October 4, 2016

U.S. DEPARTMENT OF COMMERCE
Penny Pritzker, Secretary

National Oceanic and Atmospheric Administration
Dr. Kathryn Sullivan
Under Secretary of Commerce for Oceans and Atmosphere

National Environmental Satellite, Data, and Information Service
Dr. Stephen Volz, Assistant Administrator

This page intentionally left blank

TABLE OF CONTENTS

LIST OF FIGURES

Figure 1. NCEI regional climatologies completed to date. The earliest completed climatology was the Gulf of Mexico with the climatologies placed chronologically from left to right and top to bottom. The numbers show the progression from the earliest to most recent climatologies (the most recent being the NWARC).

Figure 2. Bottom topography of the North Atlantic Ocean (ETOPO1 Global Relief Model from NOAA; http://www.ngdc.noaa.gov/mgg/image/2minrelief.html); NWARC outlines the NWA regional climatology area.

Figure 3. Scheme of the Northwest Atlantic Current System (adopted from Annual, Seasonal and Monthly Climatology of the North Atlantic web site www2.mar.dfo-mpo.gc.ca/science/ocean/woce/climatology/naclimatology.htm; courtesy of I. Yashayaev). Large white rectangle shows the NWARC domain; small rectangle roughly outlines the Mid-Latitude Transition Zone; some currents names are added; red lines show warm and cyan lines show cold currents; the convection sites in the Labrador and Greenland seas are depicted as yellow downward spirals; warm and cold Gulf Stream rings are shown as small orange and blue circles north and south of the Gulf Stream and its extension.

Figure 4. A snapshot of the surface temperature in the Gulf Stream region from (a) satellite tracking (source: NASA) and (b) sea surface temperature (SST) simulation from the NOAA Geophysical Fluid Dynamics Laboratory's (GFDL) high resolution coupled atmosphere-ocean model (source: NOAA/GFDL; http://www.gfdl.noaa.gov/visualizations-oceans).

Figure 5. Annual temperature observation density at 10 m depth for periods of (a) 1965 - 1974 and (b) 1995 – 2004 within one-degree grid boxes.

Figure 6. Annual temperature observation density at 10 m depth for periods of (a) 1965 - 1974 and (b) 1995 – 2004 within one-tenth-degree grid boxes.

Figure 7. Scheme used in computing annual, seasonal, and monthly objectively analyzed means for temperature and salinity (from Locarnini *et al.*, 2013).

Figure 8. Winter objectively analyzed temperature averaged over the years 2005-2012 at 10 m depth in three analyses on: (a) one-degree, (b) quarter-degree, and (c) one-tenth-degree grids.

Figure 9. Winter objectively-analyzed salinity averaged over the years 2005-2012 at 10 m depth in three analyses on: (a) one-degree, (b) quarter-degree, and (c) one-tenth-degree grids.

Figure 10. Winter statistical mean salinity averaged over the years 2005-2012 at 10 m depth in three analyses on: (a) one-degree, (b) quarter-degree, and (c) one-tenth-degree grids.

Figure 11. Winter minus annual objectively analyzed temperature averaged over the years 2005-2012 at 10 m depth in three analyses on: (a) one-degree, (b) quarter-degree, and (c) one-tenth-degree grids.

Figure 12. Standard error of temperature at 10 m depth for winter averaged over the period of 2005-2012 in three analyses on: (a) one-degree, (b) quarter-degree, and (c) one-tenth-degree grids.

Figure 13. Annual temperature at 10 m depth for three decades: (a) 1955-1964, (b) 1975-1984, and (c) 1995-2004.

Figure 14. Winter mean temperature at 10 m depth for three decades: (a) 1955-1964, (b) 1975-1984, and (c) 1995-2004.

Figure 15. January mean temperature at 10 m depth for three decades: (a) 1955-1964, (b) 1975-1984, and (c) 1995-2004.

Figure 16. March averages of SST for (left) 2003 and (right) 2007; SST fields are from the Remote Sensing Systems on a 0.258° grid (from Kelly *et al.* (2010).

Figure 17. January temperature at 10 m depth from (a) NWARC and (b) the NEMO numerical experiments for the decade 1985-1994.

Figure 18. July temperature at 10 m depth from (a) NWARC and (b) the NEMO numerical experiments for the decade 1985-1994.

Figure 19. Difference between decadal mean temperatures at 10 m depth from NWARC and NEMO model in January (left) and July (right) for the decade of 1985-1994.

Figure 20. RMS of difference between observed and modeled decadal temperatures at 10 m depths in January (left) and July (right) for the decade of 1985-1994 (see Figure 9).

LIST OF TABLES

ACKNOWLEDGMENTS

ABSTRACT

The Northwest Atlantic Ocean (NWA) plays a crucial role in global climate change. The Gulf Stream and North Atlantic Current System are the key elements of northward heat transport and the Meridional Overturning Circulation in the North Atlantic Ocean. The NWA includes a resource-rich coastal zone with abundant fisheries and other natural resources. Its economic significance and climatic importance resulted in many observational and research programs spanning over many decades.

To provide a more solid and improved oceanographic foundation and reference for multidisciplinary studies of the NWA, the Regional Climatology Team at the National Centers for Environmental Information (NCEI), formerly the National Oceanographic Data Center (NODC) in Silver Spring, Maryland, USA, developed a new set of high-resolution, quality-controlled, long-term annual, seasonal, and monthly mean temperature and salinity fields at different depth levels in the NWA region. This new regional climatology is based on the temperature and salinity profiles from oceanographic *in situ* observations spanning more than one hundred years archived in the World Ocean Database (WOD).

When computing anomalies from a climatology, i.e., from the temperature and salinity fields averaged over several decades, the mesoscale field is smoothed to prevent generation of spurious anomalies. The smoothing depends on the spatial grid resolution and thus can cause differences in climatological fields because of smoothing. On finer resolution grids with lesser smoothing, climatic residual of mesoscale eddies with spatial scale longer than grid cell sizes can be directly resolved and the remaining mesoscale background presumably represents the cumulative effect of mesoscale dynamics rather than a noise caused by objective analysis.

The advantage of high-resolution analysis becomes obvious as the use of shorter influence radii in the objective interpolation procedure leads to less smoothing in the region of sharp frontal zones, especially in the coastal regions. In a sense, the finer-resolution analysis pursues the same goal as using progressively reduced grid sizes did in making headway from coarse-resolution to eddy-permitting and then to eddy-resolving numerical models of ocean circulation. The high-resolution regional climatologies are closing the gaps between observations and model simulations, which allows meaningful data-model comparisons in critical data-rich regions, such as the NWA.

1. INTRODUCTION

Over the past few decades, the earth's climate system has undergone profound and rapid changes. In the last one hundred years, climatologists and oceanographers invested great effort and resources in compiling reliable climatological products based on observations and developing new generations of ocean and climate models. Together, observations and modelling provide better understanding of the state and variability of the climate system, and better ability to forecast climate changes. The applied oceanographic disciplines and applications, especially fisheries, followed this climate research effort by their own intense involvement in studying the consequences of global and local climate variability and ocean change. It is therefore instrumental to diagnose and document the past and present state of the World Ocean and its regions in order to facilitate prediction of possible future ocean and climate changes, which is especially important for the U.S with its highly developed coastal infrastructure, and for all other countries with direct access to world oceans and seas.

Understanding the coastal waters and their variability was critical for human activity and safety long before regular observations of the interior parts of the ocean basins, far from the shores, became viable. Moreover, the oceans and seas and their interaction with the atmosphere became a focal point of climate studies because of the ocean's role in the ongoing global warming (Blunden and Arndt, 2014; 2015; *Climate Change*, 2014, etc.).

Over the past century, numerous intensive ocean observational programs provided a comprehensive assessment of the ocean climatic state and its long-term variability. In the North Atlantic, there were many dozens of studies that led to a very detailed view of this part of the World Ocean. Many national and international monitoring and research programs, including the International Ice Patrol (IIP) Survey, Ocean Weather Ships (OWS), Mid-Ocean Dynamics Experiment (MODE), US-USSR POLYMODE (Polygon and MODE), World Ocean Circulation Experiment (WOCE), Climate Variability and Predictability (CLIVAR) of the World Climate Research Programme (WCRP), Rapid Climate Change Programme (RAPID) and most recently Argo − to name just a few − contributed advanced understanding of North Atlantic climate dynamics (see a review in Yashayaev *et al.*, 2015). The 21st century began with an explosion in ocean observations brought up by the advent of Argo floats (Isachsen *et al.*, 2014; Riser *et al.*, 2016; Roemmich and Owens, 2002; Roemmich *et al.*, 2009). The first Argo floats were deployed at the turn of the century, in 2000, and by October 2012 more than a million profiles of temperature and salinity were supplied. By the beginning of January 2015 the Argo array was comprised of 3,750 floats launched by 30 nations. The 'Argo Revolution' was met with great enthusiasm and immediate support by the ocean- and climate-research communities (Yashayaev *et al.*, 2015).

Argo floats were designed to overcome weather and other surface-state-related limitations (e.g., Gould *et al.*, 2004; Riser *et al.*, 2016; Toole *et al.*, 2011) to provide open-access, real-time and year-round profiles of temperature and salinity practically all over the World Ocean with a high degree of accuracy. To transmit data, Argo floats must reach the sea surface. Some Argo floats are equipped with an ice-avoidance algorithm allowing the float to detect the presence of ice as they ascend (Klatt *et al.*, 2007). It was reported that such floats operated successfully in some ice-covered environments (Wong and Riser, 2011; 2013). Ice tethered profilers also promise to overcome the problems with under-ice observations (Toole *et al.*, 2011).

There have been a few Argo floats that reported from under-ice regions in the northern Labrador Sea included in NWA, but the more southern parts of NWA are rather densely covered by Argo profiler observations (e.g., see the map of Argo coverage in Riser *et al.*, 2016). Although Argo data provides coverage away from the shelf zone and ice-covered regions, they are an important new tool for studying the open ocean in the NWA region, even if the addition of Argo data is not as substantial there compared to more remote regions, for example in the Southern Ocean.

The climate is formally defined as the ensemble of states that the major components of the planetary climate system – ocean, atmosphere, cryosphere, biosphere, landmass and its waters – transit through within a certain period, most often defined as thirty years (Monin, 1986; WMO, 2011). This time interval complies with the World Meteorological Organization (WMO) general recommendation of using 30-year periods of reference. According to this definition, the ocean is the key element of the climate system on decadal to centennial time scales. Therefore, the knowledge of the decadal changes of ocean parameters, especially temperature and salinity, is crucial for understanding and predicting climate variability on those time scales comparable to the average span of a human generation time. A key concept used in climatology is "climate normals." According to the WMO, climate normals serve as a benchmark for which recent or current observations can be compared. Practically speaking, the normals are averaged climate system parameters (temperature, salinity, pressure, etc.) within selected intervals (months, seasons, and years) over the reference 30-year periods. IMO/WMO member nations were first mandated to compute climate normals for their member countries for the 1901–30 period, and are required to update these climate normals every 30 years, resulting in the 1931–60 normals and the 1961–90 normals (Arguez and Vose, 2011). Since 1956, the WMO has recommended that each member country re-compute their 30-year climate normals every 10 years. Thus, currently the 1981-2010 is the preferred 30-year interval for computing climate normals. However, justifications for using 30-year normals for describing climate are now being questioned (Guttman, 1989; Livezey *et al.*, 2007) and there is a line of thought that a longer time interval should be used as a reference mean to compute anomalies. Therefore, in ocean heat content calculations, first published in Levitus *et al.* (2000) at the National Oceanographic Center (NODC), now the National Centers for Environmental Information (NCEI), the reference mean or base climatology was set to the entire period from 1955 to 2006, which is 50 years, i.e., much longer than the WMO-recommended 30 years to reflect the slower time scale of thermocline water (Levitus *et al.*, 2009). Currently this longer time interval is used in the routine computation of ocean heat and salt content anomalies regularly updated at the NCEI web site: www.nodc.noaa.gov/OC5/3M_HEAT_CONTENT .

In fact, the time scales of the ocean circulation, which are the key to the ocean's role in the earth climate dynamics on millennial and shorter time scales, are very different in the upper ocean, in the main thermocline, and in the deep ocean. They can also vary from years at a basin scale to hundreds of years at the global scale. The longest time scales of several centuries are determined by the global thermohaline circulation or inter-basin exchange of thermocline water (Gordon, 1986), also known as a "global conveyor" (Broecker, 1991). However, a practical approach to ocean climate diagnostics would be using a time period of sixty plus years beginning at the advent of massive ocean observations starting in the middle of the twentieth century.

There is a strong consensus among climate scientists that the main climate controls imposed on the earth's climate system by the oceans are via air-sea heat and freshwater

exchange. The oceans gain heat in the tropics and sub-tropics and release it in high latitudes. The meridional overturning circulation that regulates the poleward heat transport by ocean currents facilitates redistribution of energy between the low and high latitudes in the oceans and eventually, via air-sea interactions, in the climate system. The thermohaline structure of the World Ocean reflects all three factors – ocean-air heat exchange (controls surface water temperature), evaporation-precipitation balance (paired with melting and freezing of sea ice and river runoff, controls surface water salinity), and advection of heat and salt in the ocean by ocean currents. As ocean currents are driven by wind and density gradients, there are feedbacks, both in the ocean and atmosphere controlling the ocean-atmosphere interactions and ultimately the Earth's long-term climate state and variability. To understand and forecast ocean conditions and future changes, there is a need for ocean observations that are quality controlled and readily available to support all kinds of ocean-related research. Two main tools answering this call – the World Ocean Database (WOD) and the World Ocean Atlas (WOA) – were developed at NCEI. Additionally, a new line of products – regional ocean climatologies – has recently been established to extend the WOA capabilities even further in several selected key ocean regions.

2. WORLD OCEAN DATABASE

A more sophisticated understanding of the entire Earth climate dynamics and its long-term variability can be gained by modern climatology if ocean changes on the time scale of many decades are well understood. Therefore, the ocean-driven climate paradigm calls for developing oceanographic databases of quality-controlled historic ocean data to reveal ocean thermohaline variability on decadal and longer time scales. One of the largest and most advanced world ocean databases is the WOD compiled at NCEI, formerly NODC in Silver Spring, Maryland, USA. The first edition of the WOD was developed at NODC in 1994 and has been updated every three-to-four years since then. The updates include WOD98, WOD01, WOD05, WOD09, and WOD13 (the two digits after WOD abbreviation indicate the year when each database revision was published).

WOD contains a number of essential oceanic parameters, such as temperature, salinity, oxygen, nutrients, etc. The fundamental element of the WOD is a "cast." A cast is defined as a set of measurements for a single variable (temperature, salinity, etc.) at discrete depths taken as an instrument drops or rises vertically in the water column (Boyer *et al.*, 2013).

The hydrographic profiles in WOD are from in-situ observations collected with various oceanographic instruments. Historical oceanographic temperature data from bottle samples or "Ocean Station Data" (OSD), Mechanical Bathy-thermographs (MBT), ship-deployed Conductivity-Temperature-Depth (CTD) packages, Digital Bathythermograph (DBT), Expendable Bathythermographs (XBT), profiling floats (PFL), moored (MRB) and drifting (DRB) buoys, gliders (GLD), and undulating oceanographic recorder (UOR) profiles and historical oceanographic salinity data from OSD, CTD, PFL, MRB, DRB, GLD, and UOR profiles used in all World Ocean and regional climatology projects were obtained from the NCEI/NODC/WDC archives (WDC stands for World Data Center for Oceanography) and include all data gathered as a result of the GODAR and WOD Projects.

For climate studies, as well as for many ecosystem research projects, the key oceanographic values are temperature and salinity. With over 12 million temperature and over 5.6 million salinity profiles, WOD is the quintessential tool for assessing the long-term multi-

decadal ocean climate variability in many regions of the World Ocean. The most up-to-date release of this database, WOD13, allows computing statistics and analyses through the end of 2012. The online version of the WOD, which is being updated quarterly, is available at NCEI web site: www.nodc.noaa.gov/OC5/WOD13 .

Temperature and salinity profiles are available for download in a common format with associated metadata and quality control flags. With such abundant temperature and salinity data, WOD13 has become invaluable for characterizing ocean climate states and trend at many locations and for various time intervals. However, in many applications, there is a strong demand for analyzed rather than raw data sets available through WOD. Answering this demand, NCEI does provide such analyzed products in the form of ocean climatologies computed for the entire World Ocean and for some of its most important regions.

3. WORLD OCEAN CLIMATOLOGY

The idea of calculating and mapping long-term ocean state using all available historic oceanographic observations was first executed by Sydney Levitus. Recorded oceanographic observations in the world's oceans and seas have more than 300 years of history, yet the first detailed global ocean water property maps were compiled and published in the Climatological Atlas of the World Ocean in 1982, less than 35 years ago (Levitus, 1982). That first edition of this Atlas, known under the name of World Ocean Atlas (WOA) in all subsequent editions, was comprised of temperature, salinity, oxygen and nutrients interpolated to a regular one-degree geographical grid at 33 depth levels from the surface to 5500 meters. The monthly, seasonally and annually averaged values of those parameters over the time of several decades were called "ocean climatologies" and used as the descriptors of the climatic state (i.e., averaged over many decades) of the ocean in numerous applications thereafter.

Although WOA has become a tool of choice for many scientific groups and individuals, the community of ocean, climate and earth system modelers is perhaps one of the premier groups of users of the ocean observed climatology. At the time when the Climatological Atlas of the World Ocean was published (Levitus, 1982), two-to-one-degree spatial resolution was the limit that could be achieved with the then existed computing power and availability of data (Cox, 1975; Semtner and Chervin, 1988). In fact, in the 80s and beginning of 90s, there was a close match between the so-called non-eddy-permitting and early eddy-permitting models with sub-one-degree resolution and the WOA (there is a difference between "eddy-permitting" and "eddy-resolving" models, with the latter requiring at least one-tenth of a degree resolution; see below in this section). For example, Semtner and Chervin (1988) constrained the computed thermohaline fields between 25 m and sea surface and below 700 m in a global eddy-permitting model with half-degree resolution by restoring them to the gridded data from Climatological Atlas of the World Ocean (Levitus, 1982). It was soon found, however, that some elements of the modeled ocean climate cannot be properly resolved in ocean computer simulations with grid resolution coarser than a certain limit specific to those elements. For example, it was found that the spatial grid resolution sufficient for proper simulation of the Gulf Stream dynamics should be one-sixth of a degree or better (Chao *et al.*, 1996).

What was technically impossible only about 30 years ago, had become feasible in late 90s following a rapid surge in computing power and much better modeling skills (Maltrud and McClean, 2005; Semtner and Chervin, 1993; Semtner, 1995). With resolving ever-shorter spatial

scale processes in the ocean, climate models have greatly surpassed the one-degree WOA resolution in providing far more detailed ocean simulated climatologies. Employing finer and finer resolutions in ocean and climate models continues with an increasing pace toward fully resolved mesoscale and even shorter spatiotemporal scales of ocean and climate dynamics.

Ocean models now fall in one of three major categories – the coarse-resolution or non-eddy-permitting, eddy-permitting and eddy-resolving (Barrier *et al.*, 2015; Bernard *et al.*, 2006; Marzocchi *et al.*, 2015; Nakamura and Kagimoto, 2006). The eddy-resolving ocean models with one-tenths and/or one-twelfth degree grids are quickly replacing the eddy-permitting ocean models with horizontal grid sizes between half- to quarter-degree resolution (Barrier *et al.*, 2015; Bernard *et al.*, 2006). Coarse-resolution ocean models are becoming obsolete and are used in studies targeting qualitative rather than quantitative ocean climate simulations.

In an attempt to narrow the gap between observed and modeled ocean climatologies and to better serve the oceanographic community using NCEI ocean climatology products, quarter-degree temperature and salinity fields were first compiled by Boyer *et al.* (2005). The new WOA edition, World Ocean Atlas 2013 (WOA13) – the most recent descendant from the original Climatological Atlas of the World Ocean – was upgraded to 1/4°x1/4°-degree resolution at 102 depth levels for six decades (Locarnini *et al.*, 2013; Zweng *et al.*, 2013): World Ocean Atlas 2013 version 2 www.nodc.noaa.gov/OC5/woa13. It is a far more detailed edition than all previous releases since 1982. NCEI regional climatologies are now extending this effort to provide one-tenth of a degree resolution in several critical ocean regions.

All new regional climatologies are structured very similarly to the WOA. Compilation and analyses of regional climatology inherit all of WOA techniques and methodology.

As was mentioned above, the new class of eddy-resolving ocean models that are capable of properly resolving the mesoscale eddies and their interactions with large-scale currents are now taking the stage and will soon become a major requirement of any realistic climate forecast system. To comply with modern modeling development pace, the observed climatologies must break through the quarter-degree spatial resolution barrier and settle at one-tenth-degree or better. The main obstacle in attaining such resolutions is the lack of adequate data coverage in most parts of the World Ocean except for a few, albeit critically important, regions. In an effort to generate high-quality regional climatologies with as high spatial resolution as possible in regions that have sufficient data coverage, the NCEI Regional Climatology Projects was introduced in 2011 and is described in the following section.

4. NCEI REGIONAL OCEAN CLIMATOLOGY PROJECTS

With modern computing facilities, it would be relatively easy to generate ocean climatology on grids with very fine resolution. However, in contrast with numerical models, the grid resolution in observed ocean climatologies is restricted not by computer power, but by availability of field data. The above-mentioned eddy-resolving ocean models are capable of generating high-resolution output uniformly on any chosen grid, but high spatial resolution ocean climatology is supported by observations only in a limited number of regions of the World Ocean. Therefore, global "high resolution" ocean climatology would be such in the name only. Indeed, many grid cells in WOA13 (version 2) contain less than three observed values on the quarter-degree grid (see data distribution maps at www.nodc.noaa.gov/OC5/woa13fv2).

In contrast to the entire World Ocean, there are a few regions where data availability may support true high-resolution ocean climatologies. A new level of detail is therefore achievable, even if only regionally. Coincidentally but not surprisingly, all those regions are critically important for climate science, fishery, navigation, etc. Indeed, far more attention was directed toward better oceanographic description of those areas where humans most needed such a description.

Incidentally, the first regional climatology project had emerged and matured as a response to the urgent oceanographic research efforts linked to the Deepwater Horizon Oil Spill disaster in the Gulf of Mexico in April 2010. As a part of a wider multi-institutional project of compiling a new electronic edition of the NOAA Gulf of Mexico Data Atlas, a team of collaborators at NCEI (then NODC), created the Gulf of Mexico Regional Climatology with one-quarter and one-tenth degree resolutions. After this first implementation, other projects quickly followed: the Oceanographic Atlas of the East Asian Seas (EAS), the Arctic Regional Climatology (ARC), the Greenland-Iceland-Norwegian Seas (GINS) Regional Climatology, and, most recently, NWARC (NCEI Regional Climatologies www.nodc.noaa.gov/OC5/regional_climate). The ARC had been recently used to conduct a pilot study of the structure and variability of the ocean and seas north of 60°N (Seidov *et al.*, 2015).
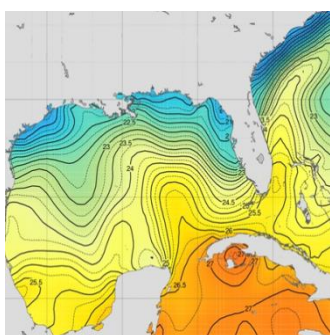
Gulf of Mexico RC (2011)   **East Asian Seas RC (2011; updated in 2015)**   **Arctic RC (2012)**
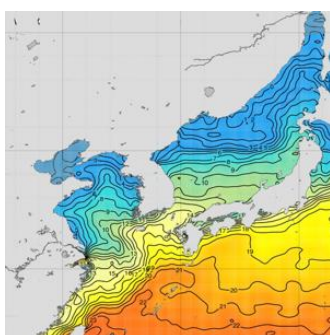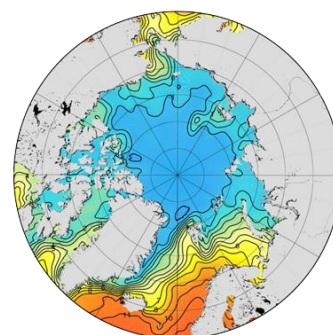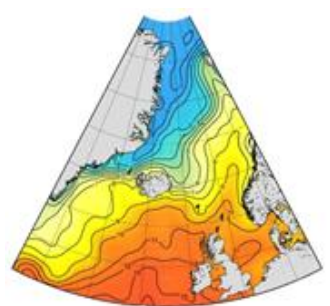
Greenland-Iceland-Norwegian Seas RC (2013)   **Climatological Atlas of the Nordic Seas and Northern North Atlantic (2014)**   **Northwest Atlantic RC (2015; updated in 2016)**
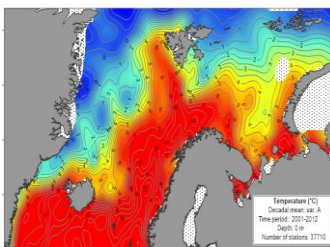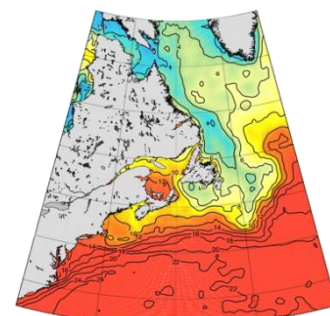
Figure 1. NCEI regional climatologies completed to date. The earliest completed climatology was the Gulf of Mexico with the climatologies placed chronologically from left to right and top to bottom (the most recent being the NWARC), with the years of first publication and updates.

All completed to date regional climatologies from the NCEI Regional Climatologies web portal www.nodc.noaa.gov/OC5/regional_climate are shown in Figure 1.

The key difference between the regional versus global climatology approach is that observed data in the selected regions have far fewer spatial and temporal data gaps to be filled by interpolation than in the vast majority of other regions of the World Ocean. Importantly, quality control on a finer spatial resolution reveals more obvious outliers than on coarser resolution grids. One of the advantages of compiling RCs is more elaborate quality control of data on higher resolution grids that it is instrumental for improving WOD and recursively WOA quality by providing additional feedback in the areas of RCs by that additional quality control on a finer grid. Yet the most important advantage of RCs is the spatial distribution of oceanographic variables retaining the sharpness of frontal zones and resolving many cumulative mesoscale features (quasi-stationary local vortices, topographic meanders, etc.; see the discussion in Chapter 11). In the next section, the advanced features of RCs will be demonstrated using the maps on one, quarter, and one-tenths of degree grids for the newest and most up to date advanced regional climatology, the NWARC.

5. NORTHWEST ATLANTIC OCEAN CLIMATE OVERVIEW

Selecting a region for compiling a regional climatology is not a trivial task. Firstly, the region should be of high importance for a number of Earth System science disciplines (e.g., oceanography, climatology, ecology, etc.), as well as for applications and allied sciences, such as fisheries, coastal engineering, coastal economics, etc. Secondly, the goal of compiling a reliable high-resolution climatology must be achievable, i.e., the density of oceanographic observations must be sufficient for such high-resolution compilation. The Northwest Atlantic is an exemplary region where the research and practical demands imposed on the needed oceanographic data are supported by data coverage. To understand why this region was selected for detailed analysis on as fine of a grid as possible based on data coverage, and to justify the NWARC project in general, some insights into major characteristics of the NWA dynamics and its climate role are outlined briefly in this and the next sections.

Climatically, the Gulf Stream System is perhaps the most important ocean current system in the World Ocean. The Gulf Steam originates as the Florida Current and flows along the US East Coast to Cape Hatteras, where it separates from the coast and becomes the North Atlantic Current. Many features of the Gulf Stream System are determined by the bottom topography and the structure of the shelf break of the western North Atlantic Ocean as shown in Figure 2. The Gulf Stream System occupies the western part of the basin.

Along the U.S. East Coast, the Gulf Stream is intensified by the northern branch of the North Equatorial Current, the warm southern Gulf Stream recirculation gyre, and the cold northern recirculation gyre. In the north, the North Atlantic Current collides with the Labrador Current to form the Mid-Latitude Transition Zone (MLTZ) east of Newfoundland and the Great Banks. The Gulf Stream System, the Labrador Sea currents, the North Atlantic Current, and the MLTZ comprise four main elements of the NWA ocean current system (Figure 3).
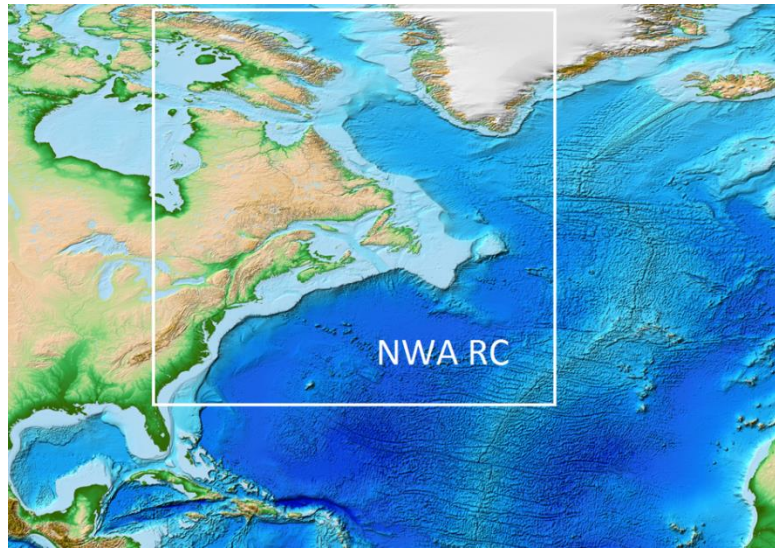
Figure 2. Bottom topography of the North Atlantic Ocean (ETOPO1 Global Relief Model from NOAA; www.ngdc.noaa.gov/mgg/image/2minrelief.html); white box outlines the NWARC domain.
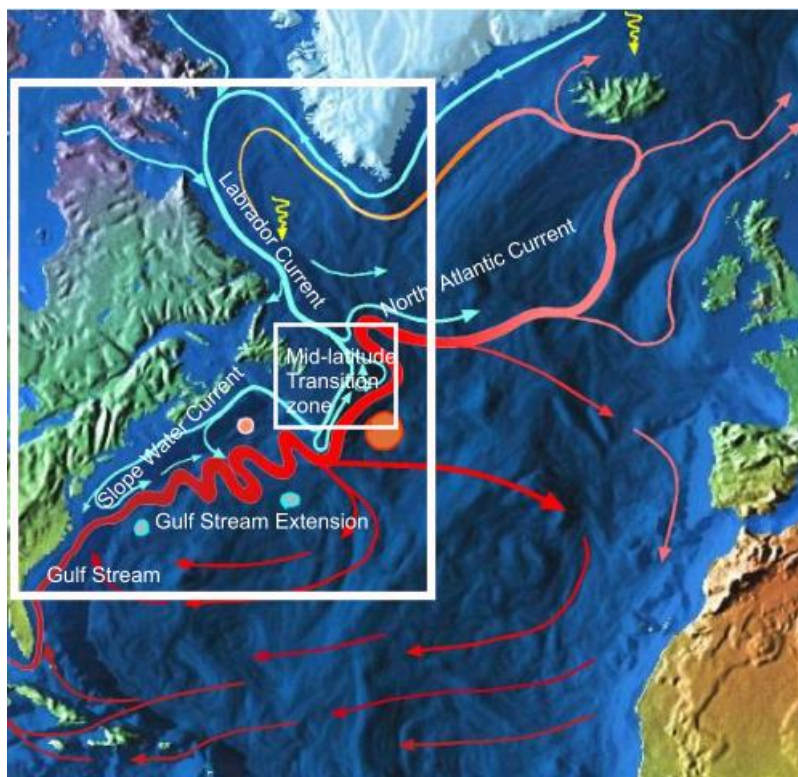
Figure 3. Scheme of the Northwest Atlantic Current System (adopted from Annual, Seasonal and Monthly Climatology of the North Atlantic web site www2.mar.dfo-mpo.gc.ca/science/ocean/woce/climatology/naclimatology.htm; courtesy of I. Yashayaev). Large white rectangle shows the NWARC domain, small rectangle roughly outlines the Mid-Latitude Transition Zone (MLTZ); some currents names are added; red lines show warm and cyan lines show cold currents; the convection sites in the Labrador and Greenland seas are depicted as yellow downward spirals; warm and cold Gulf Stream rings are shown as small orange and blue circles north and south of the Gulf Stream and its extension.

The Gulf Stream Current System is perhaps one of the most studied and charted ocean current systems to date. By the mid-20th century, oceanographers had already gained rather detailed knowledge of the Gulf Stream, especially in close vicinity to the U.S. East coast (Fuglister, 1963; Iselin, 1936; Iselin and Fuglister, 1948; Stommel, 1958). Just north of Florida Strait, there is a confluence of the Florida Current and the eastbound parts of the Caribbean and Antilles currents – two derivatives of the westbound North Equatorial Current as it reaches the Antilles Islands –the southwest-most part of the large anticyclonic subtropical ocean circulation gyre generated by the anticyclonic wind stress curl over the subtropical North Atlantic. The westward intensification of the Gulf Stream as a western boundary current is caused by the Coriolis Effect on the spherical Earth (e.g., Hogg and Johns, 1995; Munk, 1950; Stommel, 1948; 1958). The jet further intensifies between Florida Strait and Cape Hatteras by the entrainment of the water from two inner recirculation gyres to the north and south of the Gulf Stream core. The position of the stream as it leaves the coast changes throughout the year. In the fall, the core of the Gulf Stream shifts to the north, while in the spring it shifts to the south (Hogg and Johns, 1995; Schmitz and McCartney, 1993).

The two upper-ocean recirculation gyres mentioned above are the cold and warm gyres north and south of the eastbound Gulf Stream core. The cold water from the Labrador Sea flows westward along the coast (this flow is also known as the Slope Water Current). The warm water south and east of the Gulf Stream and its anticyclonic circulation around the Sargasso Sea comprises the Gulf Stream Recirculation Gyre (Hogg et al., 1986; Worthington, 1976), also known as the Worthington Gyre, between 55ºW and 75°W (Hogg et al., 1986). Both currents feed the eastbound stream and contribute to increase the Gulf Stream transport between the Florida Strait and Cape Hatteras and especially further on along the Gulf Stream Extension.

After breaking from the continental shelf, the eastbound Gulf Stream becomes the Gulf Stream Extension and continues to strengthen before it turns north at the eastern flank of the Great Banks and finally becomes the North Atlantic Current (Hogg and Johns, 1995; Wunsch, 1978). The Gulf Stream Extension is a free baroclinic jet penetrating to the ocean bottom and its structure changes from a single, meandering front to multiple, branching fronts with a great deal of mesoscale activity and increasingly large meanders. By 65°W the meandering envelope is nearly 500 km wide, which is five times the jet width at the separation point near Cape Hatteras. The water transport almost doubles downstream between Cape Hatteras and approximately 55°W resulting from the water fed by the Northern Recirculation Gyre (the Slope Water Current) and the Worthington Gyre.

The meanders and mesoscale eddies west of the North Atlantic Current comprise the MLTZ (see above) where cold and relatively fresh eastward flowing water from the Labrador Sea mixes with the warm and salty north-northeast flowing water of the Gulf Stream and North Atlantic Current (see Figure 3 above). Thus, the Gulf Stream, as a highly stratified (both vertically and horizontally) and highly unstable jet current, serves as both a barrier and a blender of warm and cold waters along its edges. Blending, or mixing, of those waters is enabled by meanders and mesoscale eddies (Bower et al., 1985). Further mixing is done by the so-called sub-mesoscale streamers that transition between eddy-induced mesoscale geostrophic mixing and smaller-scale turbulent mixing. New research shows that this type of mixing is especially important at the Cold Wall of the Gulf Stream, where the outer warm core of the Gulf Stream contacts the cold water that originated in the Labrador Sea (e.g., Gula et al., 2016; Klymak et al., 2016).

There are two types of meanders: those generated by internal dynamic instability like in a free turbulent flow, and the quasi-stationary ones caused mostly by bottom topography. The large-amplitude meanders occasionally break off from the main stream to form warm- and cold-core Gulf Stream rings (Figure 3). Anticyclonic warm core rings are found north of and cyclonic cold core rings are found south of the Gulf Stream core. The rings migrate westward and occasionally remerge with the Gulf Stream. The rings and meanders facilitate effective heat and salt exchange across the Gulf Stream frontal zone. Another source of mesoscale activity that can cause large-scale variability on longer time and space scales are the mesoscale eddies that are also known as geostrophic turbulence (Kamenkovich *et al.*, 1986; Rhines, 1979) analogous to atmospheric eddy-like motion (Charney, 1971). Nonlinear eddies are important mixing agents of the large-scale ocean circulation capable of rather efficient transport of water parcels and their associated physical, chemical and biological properties across strong frontal zones (e.g., Bower *et al.*, 1985; Bryan, 1986; Chelton *et al.*, 2011; Rhines, 2001). In general, the kinetic energy of mesoscale eddies surrounding strong jet-like currents is larger than the kinetic energy of the averaged mean flow. Those eddies are also thought to generate upscale energy flow to intensify large-scale currents (Chao *et al.*, 1996; Kamenkovich *et al.*, 1986; Richardson, 1983; Seidov, 1989; Seidov and Maruskevich, 1992). The thermohaline structure of the Gulf Stream reflects eddy-jet dynamics (Richardson, 2001). Snapshots of sea surface temperature in the Gulf Stream region using satellite imagery or eddy-resolving models show very intense mixing and turbulent structure with clearly seen mesoscale eddies, meanders and rings, as shown in Figure 4.
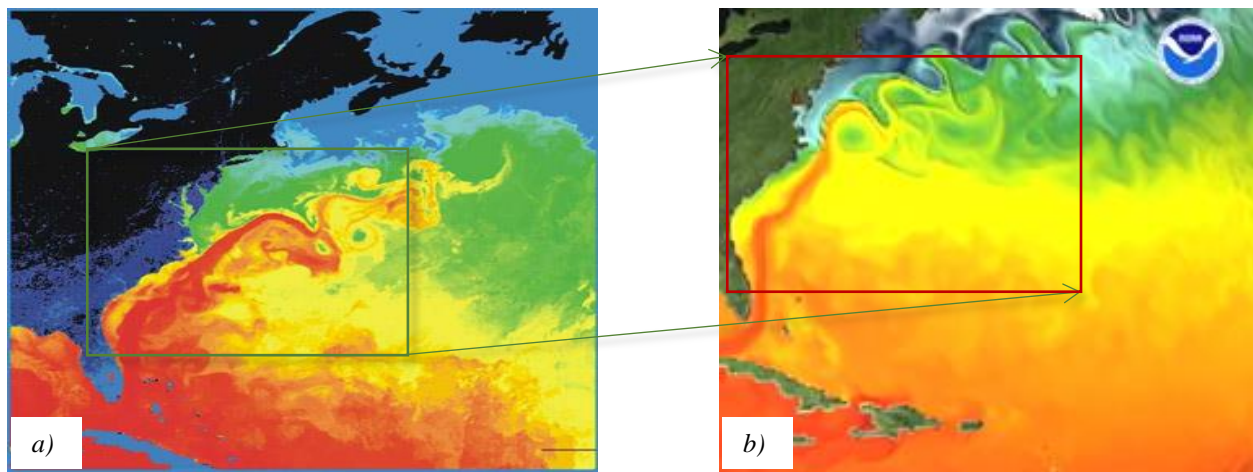
Figure 4. A snapshot of the surface temperature in the Gulf Stream region from (a) satellite tracking (source: NASA) and (b) sea surface temperature (SST) simulation from the NOAA Geophysical Fluid Dynamics Laboratory's (GFDL) high resolution coupled atmosphere-ocean model (source: NOAA/GFDL; www.gfdl.noaa.gov/visualizations-oceans).

As mentioned before, the east-northbound Gulf Stream along the North America east coast and the Gulf Stream Extension are energetic baroclinic currents with a strongly stratified warm and salty core shoaling downstream. In contrast, the east-southbound Labrador Current is much more barotropic with both upper and lower branches flowing south-east along the Canada and US eastern shelf and continental slope, known also as the Western Boundary Current or WBC (upper branch) and Deep Western Boundary Current or DWBC (deep-sea branch) of the Labrador Sea. The DWBC is the deep limb of the Atlantic Meridional Overturning Circulation – one of the key elements of global ocean circulation and one of the most important oceanic climate controls.

6. ATLANTIC MERIDIONAL OVERTURNING CIRCULATION

One of the major goals of NCEI global ocean and regional climatologies is to support ocean climate research, especially the exploration of global and regional ocean thermohaline circulation shaping the earth's global climate and thus being a focus of modern climate studies. The NWARC is specifically targeting a region fundamentally important for the entire climate system. Indeed, of all branches of the global thermohaline circulation (Gordon, 1986), also known as a "global conveyor belt" (Broecker, 1991), the most important is the Atlantic branch usually referred to as the Atlantic Meridional Overturning Circulation (AMOC). The AMOC is thought to be the most important driver of ocean climate variability on decadal and longer time scales (Bryden *et al.*, 2005; Buckley and Marshall, 2016; Delworth *et al.*, 2007; Goosse and Holland, 2005; Hu and Meehl, 2005; Srokosz *et al.*, 2012).

The AMOC's near-surface, warm northward flow is compensated by a colder southward return flow at depth. The AMOC carries warm water to high latitudes where heat loss to the atmosphere leads to the formation of the North Atlantic Deep Water (NADW) in the northern North Atlantic, Nordic and Labrador Seas. The deep southward flow of NADW comprises the deep branch of the AMOC. The strength of the AMOC and meridional heat transport are estimated as 17.2 Sv and 1.25 PW (1 Sv=10^6 m^{3}s^{-1}; 1 PW=10^{15} W) (McCarthy *et al.*, 2015); maximum transport was recorded as high as 18.7 Sv (Rayner *et al.*, 2011).

Changes in the AMOCcan contribute to regional and even global climate changes on regional and even global scale that are yet to be adequately understood. On interannual to decadal timescales, AMOC changes are primarily caused by buoyancy anomalies on the western boundary and in the MLTZ (see above), or a "western transition zone" between the subtropical and subpolar gyres (Buckley and Marshall, 2016). A decline in AMOC transport over the past couple of decades has been reported in a number of publications (Bryden *et al.*, 2005; Cunningham *et al.*, 2007; Smeed *et al.*, 2014), although some authors believe that there was no slowdown of the Gulf Stream seen in observations on a longer time scale (Rossby *et al.*, 2010; Rossby *et al.*, 2014). It is therefore instrumental to see if the interannual and decadal variability of the AMOC is manifested clearly in historical oceanographic data.

One of the important questions linked to AMOC functionality is about the large temperature and salinity anomalies in the Gulf Stream area due to the jet wobbling and path shifts. Many factors can influence the Gulf Stream path shifts, if such shift had indeed occurred on the decadal time scale. The high-resolution NWARC could be used to verify whether decadal shifts of the thermal front can be diagnosed from historic hydrographic data. As the jet width itself is on the order of ten to a hundred kilometers, the minimum resolution that is sufficient to pursuing this goal is 0.1°x0.1° or better. Thus, this is another obvious motivation for compiling a high-resolution climatology in this region.

7. NORTHWEST ATLANTIC OCEAN CLIMATE AND ECOSYSTEM DYNAMICS

The NWA is a resource-rich coastal zone with abundant fisheries and other substantial natural resources. Its economic significance and climatic importance spurred intensive observational and research programs spanning many decades. The variability of the Gulf Stream System and its connection to fisheries, and more generally to the regional marine ecosystem is now under the spotlight in many ecosystem research and review papers (e.g., Drinkwater, 2005; Drinkwater *et al.*, 2013; Holt *et al.*, 2014; Kamykowski, 2014; Sherman *et al.*, 2013, etc.).

The aquatic environments are extremely sensitive to oceanographic conditions and to ongoing ocean and climate change (e.g., Barange and Harris, 2010; Blanchard *et al.*, 2012; Mann and Lazier, 2013). Especially important are coastal zones with exceptionally high biological productivity and high rates of biogeochemical cycling (e.g., Drinkwater *et al.*, 2009; Holt *et al.*, 2009). The Northwest Atlantic in the vicinity of the U.S. and Canadian coastal zones has been the focus of intensive research linked to fisheries and ecological health of the coastal water (Barange and Harris, 2010; Shackell *et al.*, 2012; Sherman *et al.*, 2013; Skjoldal and Sherman, 2002; Stenseth, 2004). A substantial effort has been made to find connections between ecosystem dynamics and variability with large-scale ocean circulation and major climate indices such as the North Atlantic Oscillation (NAO), Atlantic Multidecadal Oscillation (AMO), etc. (Brander, 2010; Nye *et al.*, 2014; Overland *et al.*, 2010; Sarmiento *et al.*, 2004; Schmittner, 2005). Vulnerability of fisheries in the coastal zones of North America's eastern coast in response to ocean and climate change has been specifically addressed as a prime topic of fisheries-climate connections (Allison *et al.*, 2009; Brander, 2010; Jennings and Brander, 2010; Lehodey *et al.*, 2006; Sherman *et al.*, 2013).

As stated above, the NWA region is characterized by a very complex circulation pattern with fine-structured circulation and recirculation gyres, meandering jets, nonlinear baroclinic waves, meanders and rings strongly interacting with the Gulf Stream, Gulf Stream Extension, and the Labrador Current. Many research efforts point toward an intricate but clearly observed connection between biological indicators, such as chlorophyll and phytoplankton concentration and variability, and the eddy regime in the Gulf Stream System (e.g., Frajka-Williams *et al.*, 2009; Leterme and Pingree, 2008; Schollaert *et al.*, 2004). To provide a meaningful and useful observational oceanographic background for fisheries and ecosystem research, a grid resolution that is capable of resolving ocean jets, meanders, and the cumulative effects of mesoscale eddies with the grid sizes of just a few tens rather than hundreds of kilometers, is in strong demand.

Indeed, for an eddy with the size of 50 km, which is approximately half of the baroclinic Rossby wave length, one-degree resolution does not resolve this wavelength at all, while the quarter degree gives only five points per wavelength and thus provides just a borderline resolution of baroclinic eddies. The one-tenth-degree grid, on the other hand, has 8 to 10 grid points in mid-latitudes and thus provides sufficient resolution for the spatial scales of the baroclinic Rossby deformation radius. Additionally, the seasonal cycle, which may have spatial shifts of currents of tens to hundreds of kilometers, is superimposed on interannual variability and is essential for all elements of marine ecosystems (e.g., Leterme and Pingree, 2008; Skjoldal and Sherman, 2002). The decadal-scale changes in seasonal cycles are of paramount importance, especially for fish stocks in this dynamically complex and highly variable ecosystem. We can conclude, based on climate research and application demands, that selection of the NWA region for a more detailed analysis and mapping is timely and justified.

8. NORTHWEST ATLANTIC REGIONAL OCEAN CLIMATOLOGY

The NWARC domain is bounded by 80.0°W and 40.0°W longitudes and 32.0°N and 65.0°N latitudes (see Figure 2). The NWARC is comprised of analyzed temperature and salinity fields computed to map the state of the ocean in the NWA area and to assess long-term climatological tendencies in this important region. The set includes objectively analyzed temperature and salinity fields as well as some additional parameters that may be useful for

applied climate studies. These additional parameters include simple statistical means, data distributions, standard deviations, standard errors of the mean, observed minus analyzed, and seasonal minus annual distributions for both temperature and salinity.

All data from the WOD13 during the time interval between 1955 and 2012 in the NWA domain were used to calculate six decadal climatologies within the following time periods: 1955-1964, 1965-1974, 1975-1984, 1985-1994, 1995-2004, and 2005-2012 (Table 1). The averaged ~60-year climatology (*decav* – stands for *dec*adal *av*erage) was calculated by averaging the six individual decades listed above (e.g., Locarnini *et al.*, 2013). "All" climatology was computed using all data available in WOD13. Each decadal climatology consists of (a) annual (computed as the average of 12 monthly averages), (b) seasonal (winter (Jan.-Mar.), spring (Apr.-Jun.), summer (Jul.-Sep.), fall (Oct.-Dec.) computed as 3-month averages), and (c) monthly averaged fields. All monthly fields are computed as a simple average of all data available for each month within each decade. For all three grid resolutions (one-, quarter-, and one-tenth-degree), mean depth values at the center of a grid square with the respective resolution were extracted from the ETOPO2 World Ocean bathymetry.

The NWARC is designed similarly to WOA13, and therefore all characteristics of WOA13 also apply to NWARC. Hence, the following description of NWARC mostly follows WOA13 publications (e.g., Locarnini *et al.*, 2013; Zweng *et al.*, 2013). Specific features of NWARC are addressed further in the text regarding the data coverage, objective analysis, and quality control in the NWA region.

All WOA editions prior to WOA13 were comprised of analyzed oceanographic parameters at 33 depth levels with just one spatial resolution of 1°x1°. As a major upgrade, WOA13 provides objectively analyzed climatological mean and miscellaneous statistical fields on both one- and quarter-degree longitude-latitude grids with the extended vertical resolution of 102 depth levels. (Some statistical fields were computed on 5°x5° grid as well, the same as was done in previous editions). The time span of decadal fields in WOA13 stretches over six decades from 1955 to 2012 (the last "decade" – the years 2005 to 2012 – covers only eight years, whereas all other decades comprise full ten-year intervals). Table 1 shows the time spans used in both WOA13 and NWARC (see WOA13 Documentation data.nodc.noaa.gov/woa/WOA13/DOC/ woa13documentation.pdf on NCEI's web site for more details). The statistical and analyzed fields are annual, seasonal, and monthly providing a climatological year, four climatological seasons, and twelve climatological months for each decade.

Table 1. Time Spans for WOA13 and NWARC

Time Span	Abbreviation	Comment
1955 – 1964	5564	First decade with sufficient data for climatological mean fields
1965 – 1974	6574	
1975 – 1984	7584	
1985 – 1994	8594	
1995 – 2004	95A4	
2005 – 2012	A5B2	Global coverage includes Argo floats from 2005
1955 – 2012	*decav*	Average of six decadal means
All available years	all	

The procedure of computing climatological variables is as follows. Each climatological parameter (temperature, salinity, etc.) is computed as an average of each month over ten years (again, the last "decade" is over eight years). The decadal seasons are computed as the average of three sequential decadal months, beginning with winter as January-February-March, and the yearly fields computed as the average of four decadal seasons.

Table 2. Available objectively analyzed and statistical fields

Field Name	One-tenth-degree field	Quarter-degree-field	One-degree-field	Five-degree field
Objectively analyzed climatology	√	√	√	
Statistical mean	√	√	√	√
Number of observations	√	√	√	√
Seasonal or monthly climatology minus annual climatology	√	√	√	
Standard deviation from statistical mean	√	√	√	√
Standard error of the statistical mean	√	√	√	√
Statistical mean minus objectively analyzed climatology	√	√	√	
Number of mean values within radius of influence	√	√	√	

In addition to the objectively analyzed fields, both WOA13 and NWARC provide (a) statistical mean fields, (b) the observation density (number of observations in each grid cell), and (c) other statistical parameters that help to assess ocean climate on all grids as shown in Table 2. More details on time spans and other details can be found in WOA13 Documentation on the NCEI web site.

The statistical fields in NWARC were calculated for only two oceanographic variables: temperature and salinity, in contrast to WOA13 having calculations for six variables: temperature, salinity, dissolved oxygen, nitrate, phosphate, and silicate. Because different variables in the database have different levels of data coverage/data density (or sparsity), not all variables were analyzed at all depths for all averaging periods (annual, seasons and months) and time spans. Table 2 shows which fields of statistical and auxiliary variables are included in NWARC. Here is a short description of those fields:

- Objectively analyzed climatologies are the objectively interpolated mean fields for an oceanographic variable at standard depth levels for the NWA.
- The statistical mean is the average of all interpolated data values that pass quality control checks at each standard depth level for each variable in each one-tenth-, quarter-, one-, or five-degree cell which contain at least one measurement for the given oceanographic variable.

- The number of observations of each variable in each one-tenth-, quarter-, one-, or five-degree cell of the NWA at each standard depth level.
- The standard deviation from the statistical mean of each variable in each one-tenth-, quarter-, one-, or five-degree cell at each standard depth level.
- The standard error of the mean of each variable in each one-tenth-, quarter-, one-, or five-degree cell at each standard depth level.
- The seasonal or monthly climatology minus the annual climatology at each one-tenth-, quarter- or one-degree cell at each standard depth.
- The statistical mean minus the objectively-analyzed climatological mean at each one-tenth-, quarter- or one-degree cell at each standard depth. This value is used as an estimate of interpolation and smoothing error.
- The number of one-degree cells within the smallest radius of influence around each one-tenth-, quarter- or one-degree cell that contain a statistical mean value.

Table 3. Depths associated with each standard level number

Depth (m)	Level	Depth (m)	Level	Depth (m)	Level	Depth (m)	Level
0	1	250	27	1300	53	3300	80
5	2	275	28	1350	54	3400	81
10	3	300	29	1400	55	3500	82
15	4	325	30	1450	56	3600	83
20	5	350	31	1500	57	3700	84
25	6	375	32	1550	58	3800	85
30	7	400	33	1600	59	3900	86
35	8	425	34	1650	60	4000	87
40	9	450	35	1700	61	4100	88
45	10	475	36	1750	62	4200	89
50	11	500	37	1800	63	4300	90
55	12	550	38	1850	64	4400	91
60	13	600	39	1900	65	4500	92
65	14	650	40	1950	66	4600	93
70	15	700	41	2000	67	4700	94
75	16	750	42	2100	68	4800	95
80	17	800	43	2200	69	4900	96
85	18	850	44	2400	71	5000	97
90	19	900	45	2500	72	5100	98
95	20	950	46	2600	73	5200	99
100	21	1000	47	2700	74	5300	100
125	22	1050	48	2800	75	5400	101
150	23	1100	49	2900	76	5500	102
175	24	1150	50	3000	77		
200	25	1200	51	3100	78		
225	26	1250	52	3200	79		

All standard depths are shown in Table 3. However, as shown in Table 4, the monthly climatology is defined for the upper 57 levels only because of sparseness of monthly data below

1500 m. Seasonal and annual means were computed as averages of monthly fields above 1500 m and as averages of all data for seasonal fields below. The annual fields were computed by averaging the seasonal fields. There is almost no seasonal cycle signal below 1500, except for the region of deep convection, with the convection intensity depending on the seasons.

Table 4. Depth ranges and the number of standard depth levels for the statistics of temperature and salinity

Oceanographic Variable	Depths for Annual Climatology	Depths for Seasonal Climatology	Depths for Monthly Climatology
Temperature and Salinity	0-5500 meters (102 levels)	0-5500 meters (102 levels)	0-1500 meters (57 levels)

Although data coverage is much denser in the NWA region than in most regions of the World Ocean, the availability of temperature and salinity profiles varies in space and time within the NWA domain quite substantially. Tables 5 and 6 show the number of temperature and salinity profiles held in WOD13 (after automatic and manual quality control performed) within the NWA borders by months for the entire period. Thus, all temperature and salinity profiles in all casts made in every January of every year of the 1955-1964 decade are shown as January temperature and salinity profile numbers in Tables 5 and 6, respectively. The rightmost column shows all available profiles from 1955 to 2012. Note that the last "decade" of 2005-2012 is only eight years long, so the number of profiles currently available online in the quarterly updated WOD is higher.

Table 5. Number of temperature profiles in NWA region for each month of each decade from 1955 to 2012.

Temperature	1955-1964	1965-1974	1975-1984	1985-1994	1995-2004	2005-2012	1955-2012
January	8983	11448	7811	6183	4968	3169	42562
February	10863	10829	9618	7418	7033	3854	49615
March	12654	16822	13866	9941	8235	5982	67500
April	17233	18749	15991	10870	26723	7108	96674
May	21459	24126	18458	13149	33312	8353	118857
June	24191	23163	19241	13363	11190	8011	99159
July	23400	24899	19824	11426	12621	8806	100978
August	22625	25662	20183	13339	12682	9161	103652
September	18134	22860	15635	10703	11230	7219	85781
October	15534	20411	18210	11031	8592	7576	81354
November	16736	18314	15395	11192	8528	7883	78048
December	10635	10977	7164	6270	4496	4583	44125
Yearly (total)	*202446*	*228260*	*181396*	*124885*	*149610*	*81705*	*968302*

Tables 5 and 6 reveal an interesting tendency that could not have been anticipated *a priori*, namely, a decreasing number of *in situ* observations in the NWA over the period of record. Comparison of temperature and salinity by instruments gives a hint to why the number of observations in the area decreased in recent years. Tables 7 and 8 show the number of temperature and salinity profiles, respectively, for each of the six decades obtained using different instruments.

Table 6. Number of salinity profiles in NWA region for each month of each decade from 1955 to 2012.

Salinity	1955-1964	1965-1974	1975-1984	1985-1994	1995-2004	2005-2012	*1955-2012*
January	858	2396	3207	2535	2435	2543	*13974*
February	1254	2473	3308	2637	4496	2852	*17020*
March	1493	3544	5039	4176	5247	4656	*24155*
April	2976	5832	6197	5879	23493	5827	*50204*
May	2744	6393	7347	6702	29684	6664	*59534*
June	3355	6760	8073	6407	6638	6656	*37889*
July	4082	7710	10428	6703	9506	7530	*45959*
August	3910	7809	10201	7670	9371	7958	*46919*
September	2270	5573	6415	5804	8445	6038	*34545*
October	1609	4345	6717	6404	5703	6563	*31341*
November	1663	4307	5572	5271	5170	6470	*28453*
December	891	1992	2581	2821	2214	3309	*13808*
Yearly (total)	*27105*	*59134*	*75085*	*63009*	*112402*	*67066*	*403801*

As the older instruments, like MBT, left the scene and the new ones, like PFL (which is mainly Argo), entered it, the number of profiles per decade in the region changed accordingly. This is another caveat of replacing onboard measurements (e.g., from ships or stationary buys) with data from passive drifters of any type. Both are important and should be used concurrently rather that interchangeably. Argo floats, or any drifters for that matter, are not designed to target specific sites or provide specific regional coverage as they tend to disperse and follow circulation patterns rather than to remain in a selected region, as would be the case in the *in-situ* observations from ships or stationary buoys. In contrast to ship-based observations that usually targeting particular regions, the drifters tend to cover some regions more homogeneously, with lesser observation density in specific areas, which may or may be not the desired outcome depending on research goals. It should be mentioned that there might be some XBT and bottle data not having yet been reported to NCEI. However, we think that the decrease in bottle and XBT stations seen in Tables 7 and 8 is too substantial to be explained only by such an assumption.

Figure 5 shows data coverage for two decades in the NWA region on the one-degree grid. Figure 5a (left) shows the number of temperature observations at 10 m depth for the decade of 1965-1974, while Figure 5b (right) displays the number of temperature observations for 1995-2004. Figures 6a and 6b show the temperature data distribution but on the one-tenth-degree grid. (All maps showing data coverage of both temperature and salinity for all climatological months,

seasons, and years at all depths can be found at NWARC web site www.nodc.noaa.gov/OC5/regional_climate/nwa-climate).

Table 7. Number of temperature profiles in NWA region for each decade from 1955 to 2012 by instrument (see text).

Instrument	1955-1964	1965-1974	1975-1984	1985-1994	1995-2004	2005-2012	*1955-2012*
OSD	29475	59674	60317	23157	2991	734	*176348*
MBT	172971	113457	22343	15363	42		*324176*
XBT		51693	76018	44941	28443	14465	*215560*
CTD		3436	22718	41404	59194	42855	*169607*
APB						744	*744*
PFL				20	17455	21550	*39025*
UOR					41485		*41485*
GLD						1357	*1357*
Total	*202446*	*228260*	*181396*	*124885*	*149610*	*81705*	*968302*

Table 8. Number of salinity profiles in NWA region for each decade from 1955 to 2012 by instrument (see text).

Instrument	1955-1964	1965-1974	1975-1984	1985-1994	1995-2004	2005-2012	*1955-2012*
OSD	27105	55918	53973	22132	2833	737	*162698*
CTD		3216	21112	40876	58601	42747	*166552*
APB						744	*744*
PFL				1	9483	21481	*30965*
UOR					41485		*41485*
GLD						1357	*1357*
Total	*27105*	*59134*	*75085*	*63009*	*112402*	*67066*	*403801*

Note: In Tables 7 and 8 the abbreviations stand for: OSD–Ocean Station Data (bottles); MBT–Mechanical Bathythermograph; XBT–Expendable Bathythermograph; CTD–Conductivity-Temperature-Depth; PFL–Profiling Float; UOR–Undulating Oceanographic Recorder; GLD–Glider (see text), APB- Autonomous Pinniped Bathythermographs. Note that we do not show the data from MRB (Moored Buoys) because they provide large amounts of data, but in singular locations, whereas all other instruments are responsible for areal coverage (i.e., MRB are included in the NWARC, but are not shown in the Tables).

There are fewer spatial gaps between observations or empty cells in the more recent decade of 1995-2004 than in the earlier decade of 1965-1974, particularly at higher latitudes. However, the U.S. coastal area and the Gulf Stream area were noticeably better covered by observations in 1965-1974 than in 1995-2004, where many massive oceanographic programs were conducted at the early period (Yashayaev *et al.*, 2015). That is, modern technology helps to cover wider areas, especially away from the coastline, but at the expense of fewer focused observations which were characteristic of the earlier decades where intensive studies of the Gulf Stream in the 60s and 70s and mesoscale ocean eddies in the 70s and 80s occurred. On the other hand, the finer resolution is better facilitated by newer technology that helps to close the gaps and allows compiling high-resolution regional climatologies, as in the NWA case (see Tables 7 and 8). For example, the Labrador Sea is far better covered in 1995-2004 when compared to 1965-1974 (Figures 5a and 5b), with improved coverage due to the then recent introduction of Argo floats. At the same time the Gulf Stream between Florida Strait and Cape Hatteras was

better covered in 1965-1974, when many special programs of studying the Gulf Stream were conducted (compare Figures 5a and 5b). Obviously, there are more PFL profiles in 2005-2012, even though this "decade" has only 8 years covered (see Tables 7 and 8). The dispersed character of observations with passive drifters would therefore be even clearer if the 2005-2012 timeframe was used. However, because of the abridged nature of the 2005-2012 "decade" versus 1995-2004, the latter was used for more consistent comparison with another 10-year interval of 1965-1974.
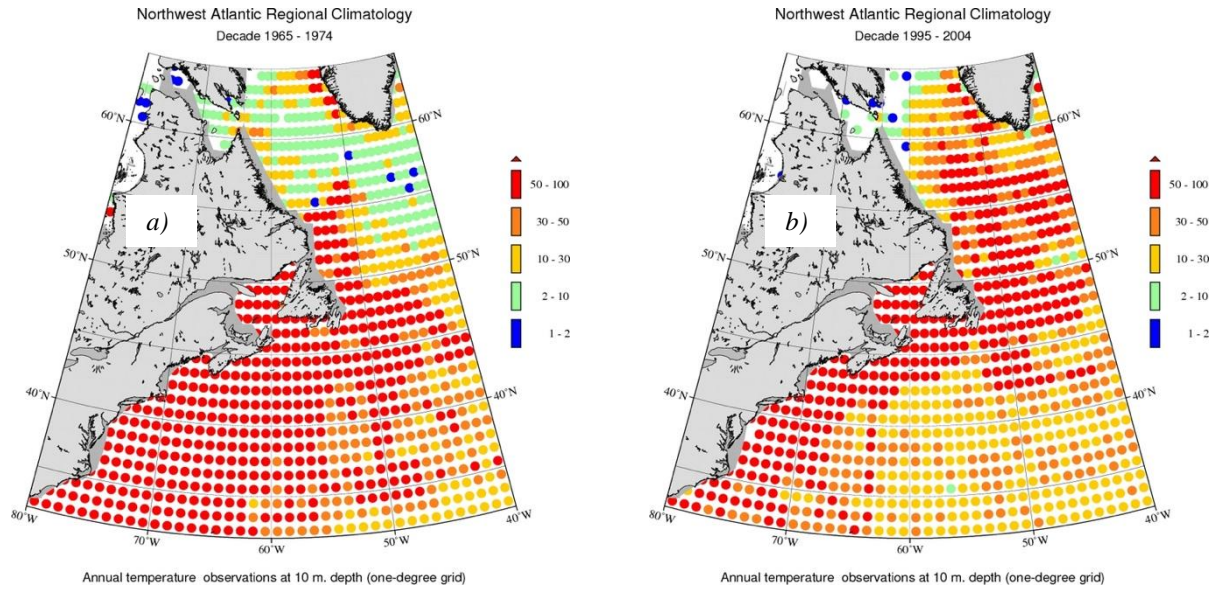

Figure 5. Annual temperature observation density at 10 m depth for periods of (a) 1965 - 1974 and (b) 1995 – 2004 within one-degree grid boxes.
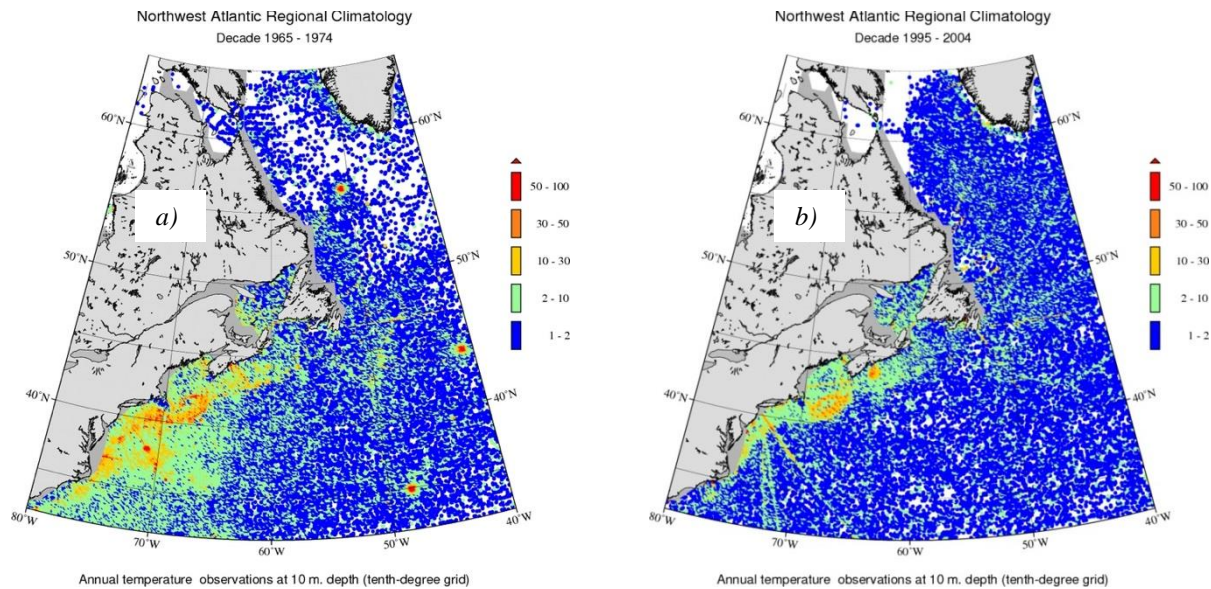

Figure 6. Annual temperature observation density at 10 m depth for periods of (a) 1965 - 1974 and (b) 1995 – 2004 within one-tenth-degree grid boxes.

29

The seasonal fields, as was stated above, are computed as the mean of three months comprising each season, and the annual fields are computed as the mean of four seasons. Such an approach mitigates, at least to some extent, possible bias toward warmer months, especially in the high latitudes. For example, even in the very well covered NWA region, there are more profiles in summer than in winter (Tables 5 and 6 above). To alleviate such a possibility, the new approach to aggregating data using climatological months to compute climatological seasons and years was used for the first time in both WOA13 and NWARC. Although monthly fields are computed at all levels and principally could have been used to calculate seasonal fields at all levels, the monthly fields are only used to compute seasonal fields in the upper 1500 m, while seasonal fields are computed using all data within a season shown below 1500 m. The caveats of using monthly and seasonal fields in the deep ocean will be discussed in the Results section.

Notably, NWARC has one-tenth-degree spatial resolution not only for annual, seasonal, and monthly temperature, but also for annual, seasonal, and monthly salinity fields for all six decades. The inclusion of six decades at such high resolution in both temperature and salinity separates NWARC from all other NCEI ocean climatology products. Moreover, in all previous regional climatologies, except for NWARC, all statistics were computed over the entire multi-decadal record only, without separation into the decadal time spans. That is, the NWA regional climatology provides, for the first time, a tool for assessing high-resolution ocean climate records based solely on historical *in situ* hydrographic observations over six decades, which is twice the WMO-recommended climate definition length.

To understand why higher resolution improves ocean climatologies, the means by which such improvements can be achieved are to be considered. In all NCEI ocean climatologies, the construct of the gridded fields is done by using the objective analysis technique. One of the most important parameters of this technique is the radius of influence (discussed in more detail in the next chapter), which essentially defines the area surrounding a grid cell from which the data are taken for interpolation to the cell center. Within the radius of influence, data points closer to the cell center are assigned higher weights. The robustness of the interpolation improves with increasing amounts of data inside the radius of influence. The radii of influence in the three-pass objective analysis on the one-tenth-degree grid is 50% to 40% shorter than on one-degree and by 34% to 13% shorter than on quarter-degree grid (e.g., Boyer *et al.*, 2005; Locarnini *et al.*, 2010; Locarnini *et al.*, 2013; Seidov *et al.*, 2015). Importantly, the radii of influence on a one-tenth-degree grid are on the scale of the Rossby baroclinic deformation radius of ~ 50 km in mid latitudes and even shorter in subpolar and polar regions. For quarter-degree resolution, the radius of influence is comparable with Rossby baroclinic deformation radius characterizing mesoscale eddies, whereas this radius is greater than the cell sizes for one-tenth-degree resolution in mid-latitudes. Having cell sizes shorter than Rossby radius facilitates better statistics and more realistic patterns in the areas with high mesoscale activity (e.g., high variance is better captured in regions such as fronts and shelf breaks).

The quality control on a higher-resolution grid reveals more outliers than an analysis on coarser resolution grids, as more observed profiles are found within fronts, stationary meanders, etc. Compared to coarser resolution, the structure of the gridded fields with one-tenth-degree-resolution is far better captured, especially in areas with sharp gradients of the essential oceanographic parameters (temperature, salinity, etc.). Such gradients and other persistent mesoscale features are better preserved in the generated climatological fields, which makes high-resolution climatologies more valuable for ocean modeling and other applications. (Importantly,

were they not persistent, mesoscale features would have been filtered out by decadal averaging, even at high spatial resolution; see the discussion in Chapter 11).

To summarize, the NWARC is a major new step toward assessing the high-resolution regional ocean climate. When compared to previous regional climatologies that provided aggregated regional climatologies averaged over the entire time span of available observations, NWARC provides six annual, seasonal and monthly decadal climatologies and presents both temperature and salinity on one-tenth-degree grid. Breaking the one-tenth degree barrier enables the NWARC to shed some important new light on decadal-scale ocean climate variability in the NWA region based on in situ oceanographic observations rather than on ocean modeling with the same (sometimes just slightly finer) resolution. Moreover, the finer resolution allows tracking changes in mesoscale features over the last six decades.

In other words, the high-resolution NWARC provides the means to study long-term thermohaline decadal variability with a grid resolution comparable with eddy-resolving numerical models of the Gulf Stream System.

9. NWARC DATA PROCESSING AND OBJECTIVE ANALYSIS

This section provides a brief summary of how profile data from WOD are processed in order to create a gridded climatology following the in-detail descriptions in the Temperature and Salinity volumes of the WOA13 (Locarnini *et al.*, 2013; Zweng *et al.*, 2013). For further information on the data sources used in WOA13 refer to the WOD13 description and user's manual (Boyer *et al.*, 2013; Johnson *et al.*, 2013). The detailed descriptions of the methods and techniques in the cited publications are fully applicable to NWARC.

To understand the procedures for taking individual oceanographic observations and constructing climatological fields, it is necessary to define the terms "standard level data" and "observed level data." We refer to the actual measured value of an *in situ* oceanographic variable as an "observation", and to the depth at which such a measurement was made as the "observed level depth." We refer to such data as "observed level data." All standard depth levels used in WOA13 and in NWARC are listed in Table 3 (see above). The procedure of interpolating data from actual depths of observations onto the standard depths is described in WOA13 documentations (e.g., Boyer *et al.*, 2013; Locarnini *et al.*, 2013).

Quality control of the temperature and salinity data is a major task, the difficulty of which is directly related to lack of data and metadata upon which to base statistical checks. The quality of oceanographic datasets and their usability for a given application critically depend on the data coverage. Data coverage as used here is not just the volume of data in the region as a whole, but refers particularly to the spatial distribution of data, which is the key indicator of the quality of the data set used to obtain climatological means. The data coverage differs hugely in different regions of the World Ocean. Thus, the success of compiling a meaningful and useful regional climatology critically depends on how much data are available and how they are distributed in a selected domain. Fortunately, as was mentioned above, the NWA region is one of the best-covered regions of the World Ocean thus giving hope to compiling a meaningful high-resolution regional decadal climatology. It can therefore be anticipated that NWARC will provide solid oceanographic foundation for ocean climate studies and numerous practical applications with embedded dependencies on long-term ocean climate change.

The data used in ocean climatology calculations need to be pre-processed to ensure quality of the gridded and analyzed fields. First, duplicate profiles and obvious outliers have to be removed prior to visual inspection and final manual quality control preceding climatology compilation. Because both temperature and salinity data are received from many sources, sometimes the same data set is received at the NCEI archive more than once but with slightly different time and/or position and/or data values, and hence are not easily identified as duplicate stations. To eliminate the repetitive data values, WOD is constantly being checked for the presence of exact and "near" exact duplicates using a minimum of eight different criteria. The first checks involve identifying stations with exact position/date/time and data values; the subsequent checks involve offsets in position/date/time and data. Profiles identified as duplicates in the checks with a large offset were individually verified to ensure they were indeed duplicate profiles.

Range checking (i.e., checking whether a measured value is within a preset minimum and maximum value as a function of depth and ocean region) was performed on all temperature and salinity values as a first quality control check to flag and withhold from further use the relatively few values that were grossly outside expected oceanic ranges. The procedure is detailed in Johnson *et al.* (2013).

As summarized in WOA13 publications (e.g., Locarnini *et al.*, 2013), first the five-degree square statistics were computed, and the data flagging procedure was used to provide a preliminary data set. Each five-degree square box was designated as coastal, near-coastal, or open ocean, depending on the number of one-degree latitude–longitude grid boxes in the five-degree box which were land areas. The data exceeding three, four, and five standard deviations in the open-ocean, near-coastal and coastal areas, respectively, were flagged as not to be included in computing and re-computing the climatology.

After the first cleaning of data is completed and outliers marked, the one-degree square statistics are computed, and the data flagging procedure described above was used to provide a preliminary data set. Next, new one-degree-square statistics were computed from this preliminary data set and used with the same statistical check to produce a new, cleaner data set. The reason for applying the statistical check twice was to flag (and withhold from further use), in the first round, any grossly erroneous or non-representative data from the data set that would artificially increase the variances. The second check is then more effective in identifying values with smaller differences that are still non-representative.

Each cast containing both temperature and salinity was checked for static stability, E, as used by Lynn and Reid (1968) and is given by:

$$E = \lim_{\partial z \to 0} \frac{1}{\rho_0} \frac{\delta \rho}{\partial z} \qquad (1)$$

where: $\rho_0 = 1.02 \ kg \cdot m^{-3}$.

As noted by Lynn and Reid (1968), static stability "is the individual density gradient defined by vertical displacement of a water parcel (as opposed to the geometric density gradient). For discrete samples the density difference ($\delta \rho$) between two samples is taken after one is adiabatically displaced to the depth of the other". For the results at any standard level (k), the computation was performed by displacing parcels at the next deeper standard level (k+l) to level k.

The final and most time-consuming step in pre-processing the data to build a decadal or any other climatology is subjective manual flagging of data, where the so-called "bullseyes" are detected and flagged to filter the data from part of the profile and sometime the entire profile from subsequent recalculation of the climatology, or "climatology re-run." Analysis for NWARC was done on three grids: a one-, a quarter-, and a one-tenth-degree grid. For the one-degree analysis, the temperature and salinity data were averaged by one-degree cells for input to the objective analysis program. After initial objective analyses were computed, the input set of one-degree means still contained questionable data contributing to unrealistic distributions, yielding intense "bullseyes" or unrealistic spatial gradients. If bullseyes or unrealistic gradients were found the data were flagged. The procedure was repeated for the quarter- and one-tenth-degree grids.

After subjective manual quality control procedures were completed on all grids for all decades, the new first guess field was calculated on a one-degree grid and then all climatologies were recomputed and the objective analysis was performed on all grids and all accompanied statistics were recalculated. The first-guess field for each of these climatologies is the "all-data" temperature and salinity fields. Zonal mean fields are used for compiling one-degree fields. Then one-degree fields are used as the first-guess field for compiling one-quarter- and one-tenth degree fields. Usually, the entire step of manual quality control and subsequent climatology re-run was repeated several times to ensure the best possible quality within reasonable time and effort.

Data processing procedures comprise the entire sequence of steps resulting in compiling climatology or a set of climatologies. The WOA13 and NWARC contain six decadal climatologies, *decav* (the average of six decadal climatologies), and the long-term average of all data or the "all-data" climatology). Compilation of the climatologies consists of several technical sub-procedures described in depth in a number of WOA publications (e.g., Belkin *et al.*, 1998; Boyer *et al.*, 2005; Levitus *et al.*, 2012; Locarnini *et al.*, 2013; Zweng *et al.*, 2013).

The objective analysis scheme adopted for all editions of WOA since WOA98 was introduced in Barnes (1964) and then updated in Barnes (1973) and Barnes (1994). As recommended in Barnes (1994), multi-pass analysis (three passes have been used in all WOA editions since WOA98 and in NWA regional climatology) was used to prevent the creation of artificial fronts, as happened in WOA94, when single-pass analysis was used (Locarnini *et al.*, 2010).

The NWARC, like all previous versions of WOA and regional climatologies, was built using a procedure widely known in geophysics as objective analysis of irregularly distributed data (Thomson and Emery, 2014). Here, a brief description of the objective analysis scheme implemented at NCEI is described. A three-pass correction is used that begins with a ''first-guess'' field, which are zonally averaged temperature or salinity fields for each one-degree latitudinal belt split by ocean basins; in NWA case the North Atlantic zonally-averaged values are used. The second step is finding all data that are available within an influence radius around the center of the grid cell being analyzed. The correction to the first-guess values at all grid points is then computed as a distance-weighted mean of all grid point difference values that lie within the influence radius. This correction procedure is repeated twice more, each time with a decreasing search radius, for a total of three passes.

The goal of the entire procedure is to fill all gaps and produce relatively smooth yet realistic fields of ocean variables on a regular grid. The influence radius is different for different grid resolutions and varies from 892 km to 154 km in the three-pass objective interpolation procedure for one, one-fourth and one-tenth degree grids respectively (see Table 9; more detailed explanation in the next section). Thus, as seen in Table 9, the influence radius in one-tenth-degree resolution is 30% shorter than the quarter-degree one, which allows influence from a more geographically compact region with finer resolution of the objectively analyzed field, if the data availability is high (as in most regions of the NWA). In a way, if compared to numerical models, shortening the radius of influence is similar to decreasing the lateral turbulent mixing causing smoother current and hydrography structures.

Table 9. Radii of influence used in objective analysis for one-degree, quarter-degree, and one-tenth-degree NWA climatologies.

Pass Number	1° Radius of Influence	1/4° Radius of Influence	1/10° Radius of Influence
1	892 km	321 km	253 km
2	669 km	267 km	198 km
3	446 km	214 km	154 km

More details about the objective analysis scheme used to generate the climatological fields can be found in the WOA documentation (Antonov *et al.*, 2010; Locarnini *et al.*, 2010; Locarnini *et al.*, 2013; Zweng *et al.*, 2013) and in the related publications (e.g., Boyer *et al.*, 2005; Levitus *et al.*, 2012). In addition to the WOA documentation cited above, the mathematical background of the technique is revisited in the Appendix of the above cited publication by Levitus *et al.* (2012). The Appendix in Levitus *et al.* (2012) also provides a description of how the statistical errors of an objectively analyzed gridded field can be estimated using a general formula for error propagation (Taylor, 1997).

In NWARC, the analysis was performed on the one-, quarter-, and one-tenth-degree grids. Inputs to the analysis scheme were one-degree grid cell means of data values at standard levels (for time period and variable being analyzed), and a first-guess value for each cell. For instance, grid-cell means for our "all-data" annual analysis were computed using all available data regardless of date of observation. For "all-data" July, all historical July data regardless of year of observation were used. For "decadal" July, only the data collected in July within a specified decade were used.

Importantly, the influence radius, and the number of five-point smoothing passes can be varied in each of the three sequential iterations in the three-pass variation of the implemented objective analysis procedure. The strategy is to begin the analysis with a large influence radius and decrease in each of the subsequent iterations. This technique allows analyzing of progressively smaller scale phenomena in subsequent iterations.

After computing the first-guess fields, the temperature and salinity data were re-analyzed using the newly produced analyses as first-guess fields described as follows. As was mentioned above, a new annual mean was computed as the mean of the twelve monthly analyses for the upper 1500 m, and the mean of the four seasons below 1500 m depth. This new annual mean was used as the first-guess field for new seasonal analyses. These new seasonal analyses in turn were used to produce new monthly analyses yielding slightly smoother means. These so-called "time-

indeterminate" monthly mean objectively analyzed temperature fields were used as the first-guess fields for each of the "decadal" monthly climatologies. Likewise, time-indeterminate seasonal and annual climatologies were used as first-guess fields for the seasonal and annual decadal climatologies.

In some cases, data-sparse regions are so large that a seasonal or monthly analysis in these regions is meaningless. On the contrary, the geographic distribution of observations for the "all-data" annual periods (for example, see appendices in Locarnini *et al.*, 2013) has very little gaps and for the task of objective analysis it covers the World Ocean almost entirely. For the NWA region, the data distribution for "all-data" is especially dense, at least in the upper layers of the ocean. By using an "all-data" annual mean first-guess field, regions where data exist for only one season or month will show no contribution to the annual cycle. By contrast, if we used a zonal average for each season or month, then, in those latitudes where gaps exist, the first-guess field would be heavily biased by the few data points that exist. If these were anomalous data in some way, an entire basin-wide belt might be affected.

One advantage of producing "global" fields for a particular compositing period (even though some regions are data-sparse) is that such analyses can be modified by investigators for use in modeling studies. Moreover, the descendant regional climatologies, in this case the NWARC, use more "time-granular" fields that are another strong advantage of the granular global approach.

For the quarter- and one-tenth-degree first-guess field, the one-degree time-indeterminate field was used. Each of the sixteen quarter-degree boxes enclosed used the one-degree time-indeterminate value as a first-guess, thereby projecting the one-degree climatology onto the quarter-degree grid. Similarly, each of the hundred one-tenth-degree boxes used the same time-indeterminate one-degree value as a first guess, thereby projecting on-degree climatology onto the one-tenth-degree grid. In those areas where there was no one-degree value due to land or bottom mask, the statistical mean for the entire basin at the given depth was used.

Special care is needed near the domain boundaries (i.e., coastlines and the ocean bottom). Thus corresponding masks are to be used while gridding the data. The analyses employed in the NWARC use ETOPO2 land-sea topography to define ocean depths at each grid-point (ETOPO2, 2006). From the ETOPO2 land mask, a quarter-degree land mask was created based on ocean bottom depth and land criteria. The details of the masks in the WOA13 can be found in (Locarnini *et al.*, 2013).

The workflow of computing NWARC seasonal and annual fields that includes density stabilization briefly outlined in this chapter is shown in Figure 7. Detailed discussion of the entire processing cycle can be found in Locarnini *et al.* (2013) and in Zweng *et al.* (2013).

As was mentioned above, the density field computed using temperature and salinity must be stabilized. Temperature and salinity climatologies are calculated separately, as there are some profiles with salinity measurements that are not always paired with temperature measurements. As a result, when density is calculated from standard level climatologies of temperature and salinity, instabilities may result in the vertical density field (stability defined in previous section). While instabilities do occur in the ocean on an instantaneous time frame, these instabilities are usually short-lived and not characteristic of the mean density field. The stabilization of density is done globally in WOA and thus is not described here in detail. The Appendices A (Section 8.1) and B (Section 8.2) in Locarnini et al. (2013) describe a technique that was employed to

35

minimally alter climatological temperature and salinity profiles to achieve a stable water column everywhere in the world ocean. The technique is based on the method of Jackett and McDougall (1995). The final temperature and salinity climatologies reflect the alterations due to this process.
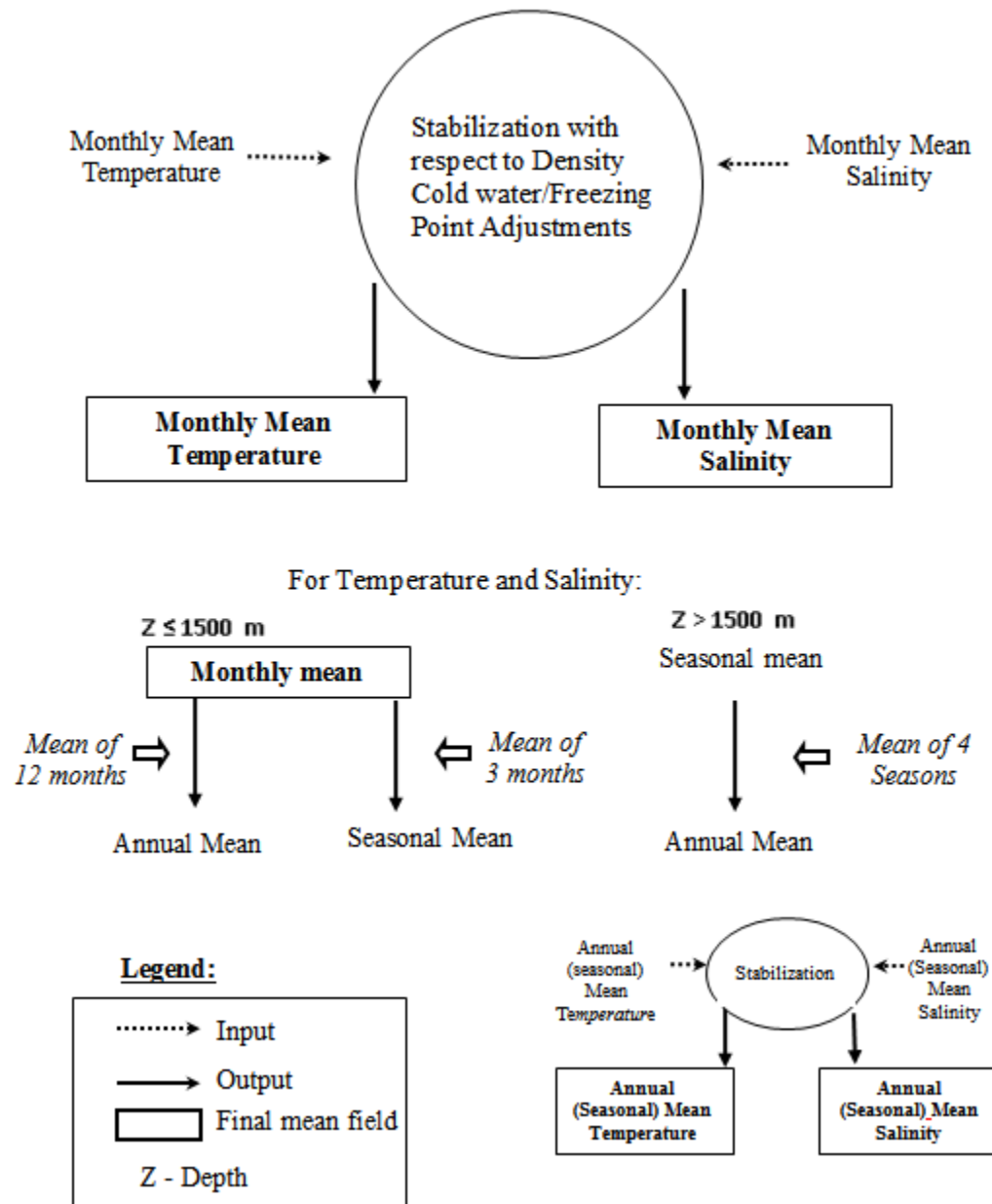

Figure 7. Scheme used in computing annual, seasonal, and monthly objectively analyzed means for temperature and salinity (from Locarnini *et al.*, 2013).

10. ONLINE NWARC MAPS AND DATA

The maps are arranged by composite periods: annual, seasonal, and monthly. The complete set of all climatological maps, objectively analyzed fields, and associated statistical fields at all standard depth levels are available online.

The sample standard deviation in a grid-box was computed using:

$$s = \sqrt{\frac{\sum\limits_{n=1}^{N}(x_n - \bar{x})^2}{N-1}} \qquad (2)$$

where x_n = the n-th data value in the grid-box, $\bar{x}$ = mean of all data values in the grid-box, and N = total number of data values in the grid-box. The standard error of the mean was computed by dividing the standard deviation by the square root of the number of observations in each grid-box.

All objectively analyzed fields and all statistical data fields can be obtained online in ASCII comma-separated value format (.csv), netCDF (.nc), and ArcGIS (.shp) formats through the NWA regional climatology webpage http://www.nodc.noaa.gov/OC5/regional_climate/nwa-climate/. For users interested in specific geographic areas, the World Ocean Atlas Select query tool (WOA*select*: www.nodc.noaa.gov/OC5/SELECT/woaselect/woaselect.html) can be used to designate a desired geographic area, depth, and oceanographic variable to view, and optionally to download. This includes climatological means or related statistics in shapefile format, which is compatible with ESRI ArcGIS and other GIS software. For users interested in other NCEI RCs completed to date, they can be found at NCEI regional climatology webpage www.nodc.noaa.gov/OC5/regional_climate. A pilot study was published by Seidov *et al.* (2015) which shows an example of using these new high-resolution regional climatologies in oceanographic research. Table 2 (Section 8) lists all objective and statistical fields included in the NWA regional climatology set.

All of the maps use consistent symbols and notations for displaying information. Continents are displayed as light-grey areas. Oceanic areas shallower than the standard depth level being displayed are shown as solid gray areas. The objectively analyzed distribution fields include the nominal contour interval used. In addition, these maps may include in some cases additional contour lines displayed as dashed black lines. All of the maps were computer drafted using Generic Mapping Tools (Wessel and Smith, 1998).

The online maps for this atlas include seven types of horizontal maps representing annual, seasonal, and monthly spatial distribution of analyzed data and data statistics as a function of selected standard depth levels for temperature and salinity:

1. Objectively analyzed temperature climatology fields. One-, quarter-, or one-tenth-degree grids (as applicable) for which there were less than three values available in the objective analysis defined by the influence radius are denoted by a white "+" symbol.

2. Statistical mean temperature fields.

3. Data distribution fields for the number of temperature observations in each one-, quarter-, or one-tenth-degree latitude-longitude grid cell used in the objective analysis binned into 1-2, 3-5, 6-10, 11-30, 31-50 and greater than 51 observations ranges.

4. Standard deviation fields binned into several ranges depending on the depth level. The maximum value of the standard deviation is shown on the map caption.

5. Standard error of the mean fields binned into several ranges depending on the depth level.

6. Difference between observed and analyzed fields binned into several ranges depending on the depth level.

7. Difference between seasonal/monthly fields and the annual mean field.

It is important to note that the high-resolution monthly temperature and salinity data coverage on the one-tenth-degree grid have more gaps than seasonal and annual fields computed from the monthly fields. In general, all high-resolution analyzed fields should be reviewed carefully before using them in mission-critical applications. It is especially important when working with the high-resolution monthly fields. Users are advised to review the data distribution and statistical mean maps before deciding whether to use the high-resolution analyzed temperature and salinity fields or their climatological means. Moreover, the monthly maps of objectively analyzed data on one-tenth-degree grid may show some possibly spurious eddy-like irregularities in some regions due to interpolation and plotting artefacts combined. Although such cases are very few, a more careful review of the fields with such occurrences is needed before using analyzed variables in research or applications.

Displaying only monthly fields that are shallower than 1500 m requires more explanation. Indeed, we do not know how deep the seasonal signal can penetrate into the ocean. Were the mixing in the ocean only limited to the upper mixed layer with turbulent diffusion below that layer, the seasonal signal would be confined to the upper several hundred meters. In most of the ocean volume this would probably be true, but in regions of strong upwelling and convection, especially seasonal deep convection in high latitudes, seasonal variability can penetrate quite deep, which is seen in the analyzed fields. On the other hand, the scarcity of data at the depths below 1500 m makes any seasonal analysis questionable, at the very least. It may soon improve, as Argo floats become more abundant, but for the time being the data below 1500 m in the NWARC area are still noticeably scarcer compared to the upper ocean. Thus, a reasonable solution was to show decadal monthly fields above 1500 m only. Although seasonal fields are shown below 1500 m, they should be considered rather cautiously. In contrast, the aggregated annual fields computed by averaging all data can be deemed as more reliable than "seasonal" fields, as additional smoothing is applied while averaging over the four seasons. This issue needs a more careful consideration in future research in order to determine how variability in the deep ocean is to be treated.

11. RESULTS AND DISCUSSION

The most important feature of the new NWA fine resolution regional climatology is the six-decade timespan, which makes NWARC a useful tool for assessing ocean long-term variability. Notably, although spatial and temporal changes can be assessed to some degree using the WOA13 on the quarter-degree grid, many features of the NWA regional ocean climate dynamics cannot be evaluated properly because the spatial scales of the processes in this region cannot be adequately represented on the grid coarser than one-tenth of a degree (or better, if possible). Figures 8 and 9, showing winter temperature and salinity for the nearly decadal

interval of 2005-2012, provide the examples of difference in climatologies with different resolutions.

In general, an important difference gained by using fine spatial resolution, obvious in Figures 8 and 9, is that the Gulf Stream and Gulf Stream Extension features are more coherent in one-tenth degree analysis than in the quarter-degree one, and of course far more coherent than in the analysis on the one-degree grid. All frontal zones are noticeably narrower on the finer grid and far better reflect the cumulative effects of mesoscale dynamics characteristic for this area.

One feature of the fine-resolution maps that really stands out in Figures 8 and 9 is the Gulf Stream structure in the southwest corner of the domain. The jet is highly coherent and parallel to the continental shelf break in the one-tenth of a degree case (Figures 8c and 9c), while even on the quarter-degree grid this pronounced jet character is completely lost. The slope water north of the Gulf Stream Extension is also better resolved on the finest-resolution grid. The Gulf Stream is about twice narrower than in quarter-degree maps and is up to three to four times narrower if compared to one-degree plots.
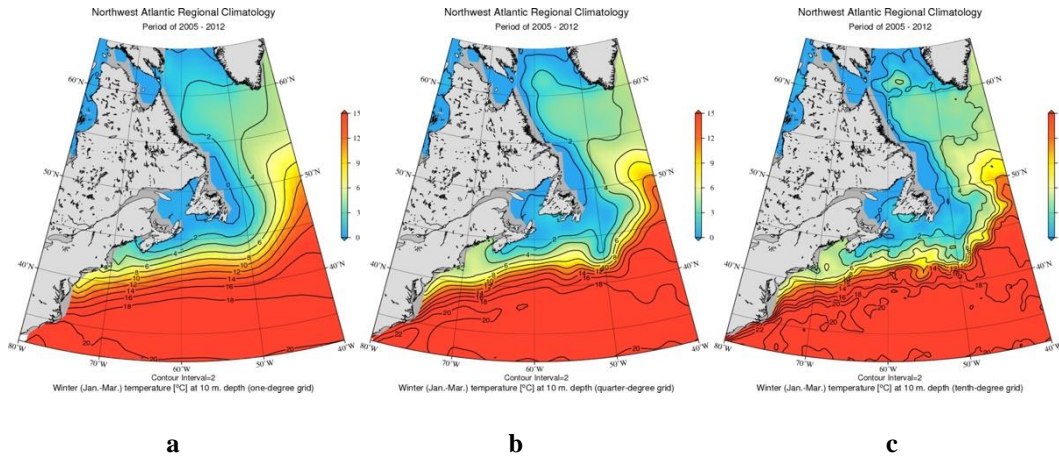

Figure 8. Winter objectively analyzed temperature averaged over the period of 2005-2012 at 10 m depth in three analyses on: (a) one-degree, (b) quarter-degree, and (c) one-tenth-degree grids.
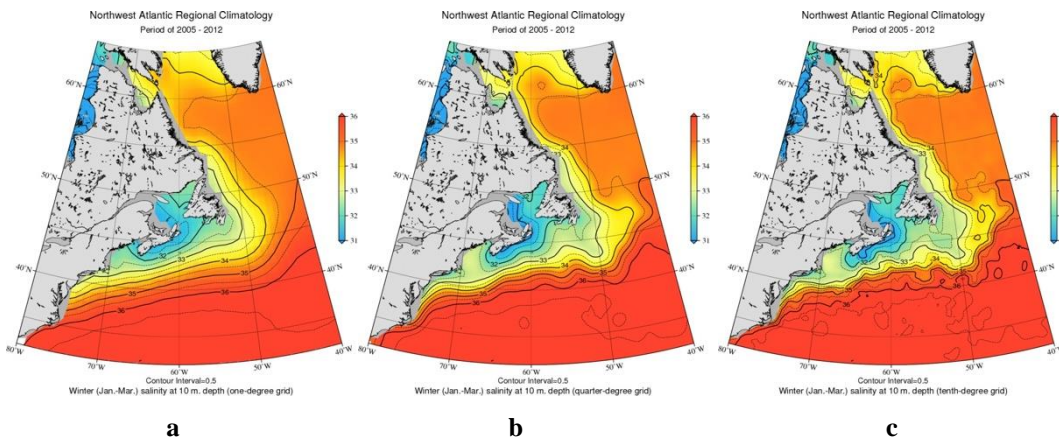

Figure 9. Winter objectively-analyzed salinity averaged over the period of 2005-2012 at 10 m depth in three analyses on: (a) one-degree, (b) quarter-degree, and (c) one-tenth-degree grids.

Stepping up in resolution to one-tenth-degree allows locating the correct position of the jet separation from the shelf at Cape Hatteras (see the discussion in Holt *et al.*, 2014) and to picture a more complex and realistic MLTZ. A clearer representation of the cold and fresh water carried by the Labrador Current south of Nova Scotia along the New England shelf with one-tenth-degree resolution is obvious when compared to one-degree or quarter-degree resolutions. The Slope Water Current looks better aligned in its recirculation path to form the Gulf Stream "northern wall" (Frankignoul *et al.*, 2001; Joyce *et al.*, 2013). Salinity in Figure 9c shows the frontal features similar to the thermal front (to form the density front of the same quality) shown in Figure 8c and it is well pronounced and narrow, as usually seen in advanced eddy-resolving numerical models.

The temperature and salinity shown in Figures 8 and 9 were computed using the objective analysis technique, which, while indisputably powerful, has its own weaknesses, as have all interpolation techniques; in particular, it may generate artificial features if the gaps between data filled cells are too numerous. As the NWA is a region rather densely covered by observations, the simple statistical mean can be used to assess the quality of the objectively-analyzed fields in this domain (Figure 10).
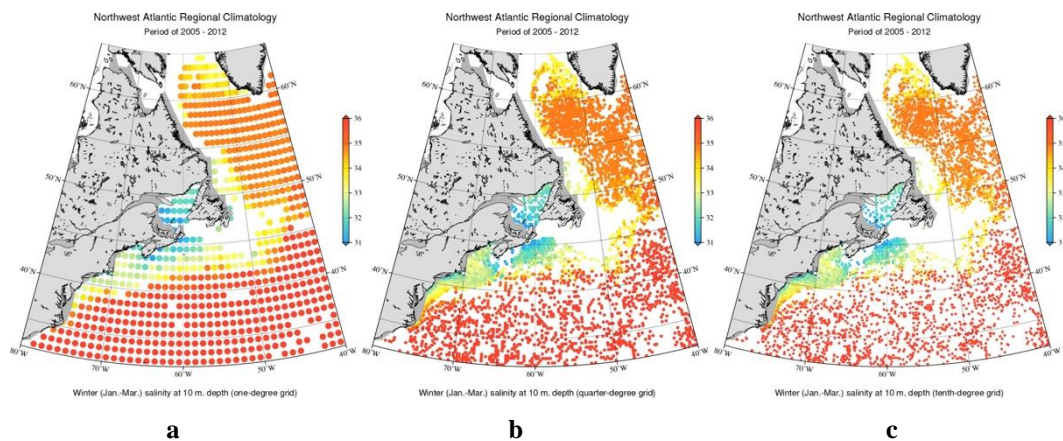

Figure 10. Winter statistical mean salinity averaged over the period of 2005-2012 at 10 m depth in three analyses on: (a) one-degree, (b) quarter-degree, and (c) one-tenth-degree grids.
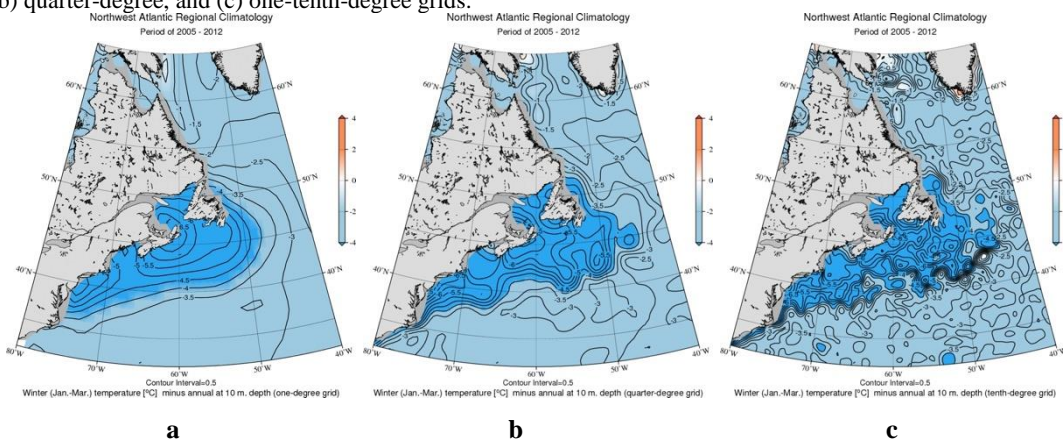

Figure 11. Winter minus annual objectively analyzed temperature averaged over the period of 2005-2012 at 10 m depth in three analyses on: (a) one-degree, (b) quarter-degree, and (c) one-tenth-degree grids.

The Gulf Stream seasonal shift and Slope Water invasion during the winter season is more pronounced in one-tenth-degree analysis, which supports the general understanding of winter jet intensification, especially in the Gulf Stream Extension (e.g., Taylor, 1996; Marshall and Nurser, 1988).

Finally, the standard error of the mean is noticeably reduced in many places on the finer grid, as can be expected. Indeed, the standard error for the three resolutions (the same time interval and depth as in all other maps above) shows substantial improvement at the finer grids, especially in the Gulf Stream area from Florida Strait up to Nova Scotia and in the Labrador Sea (Figure 12).
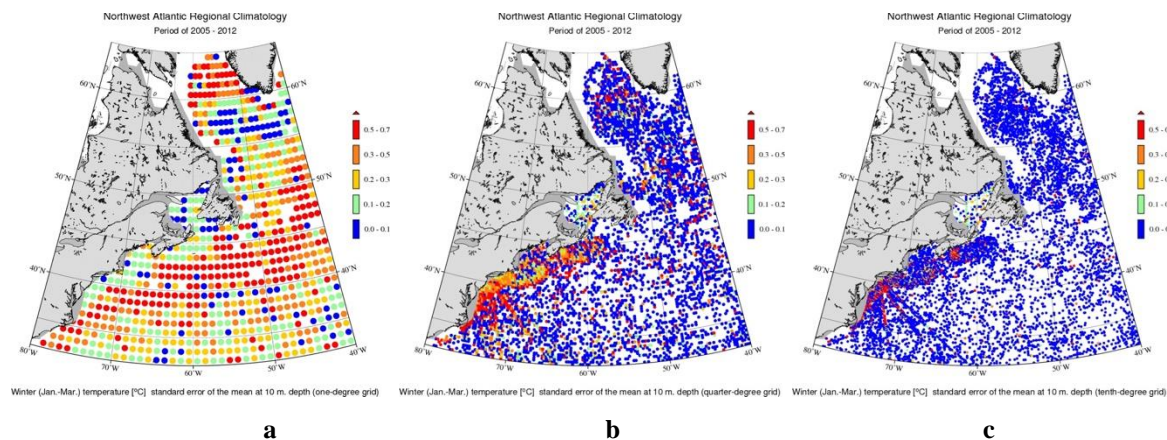

| a | b | c |

Figure 12. Standard error of temperature at 10 m depth for winter averaged over the period of 2005-2012 in three analyses on: (a) one-degree, (b) quarter-degree, and (c) one-tenth-degree grids.

Subsequent analyses of the climatological fields in the NWA region, such as decadal variability of temperature, salinity, and ocean heat and salt content, are needed and may be the subject of a follow-up publication.

| a | b | c |

Figure 13. Annual temperature at 10 m depth for three decades: (a) 1955-1964, (b) 1975-1984, and (c) 1995-2004 on one-tenth-degree grid.

There is a fundamental issue about the observed decadal climatologies regarding the "cumulative" mesoscale effects, or the mesoscale activity averaged over a decadal timespan. The seasonal variability is stronger than the mesoscale variability, which is confirmed when

41

reviewing the annual climatologies for any decade. Figure 13 shows the annual temperature climatologies for three decades. Temperature at 10 m depth for winter and January for the same three decades is shown in Figures 14 and 15.
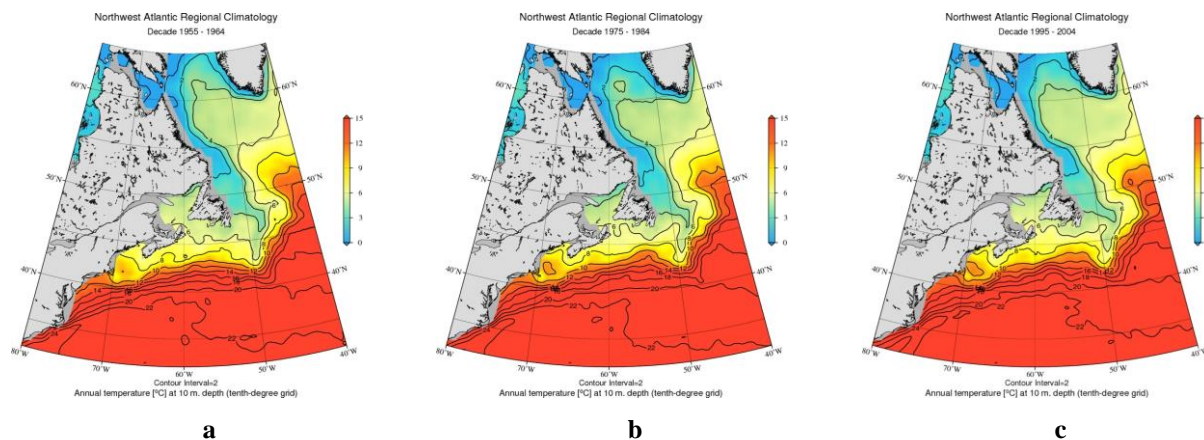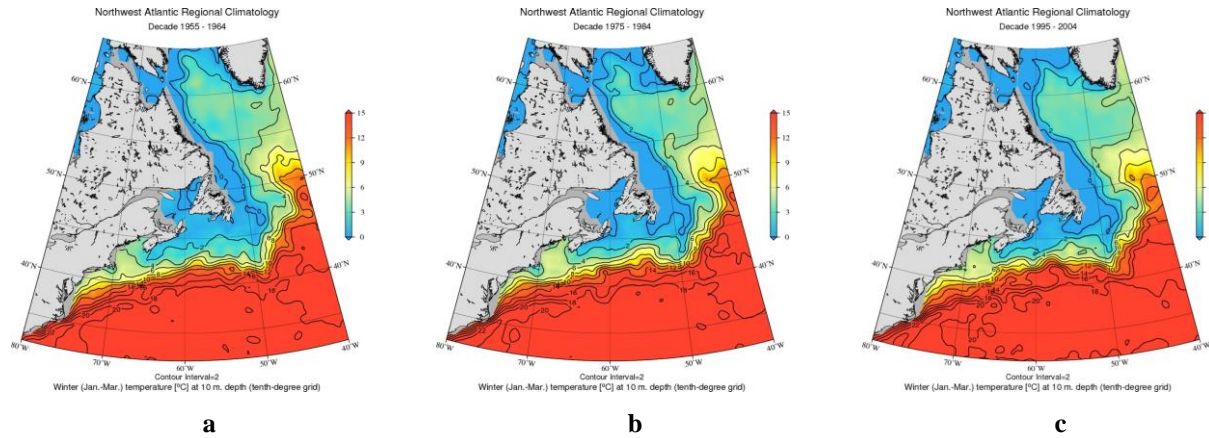

Figure 14. Winter temperature at 10 m depth for three decades: (a) 1955-1964, (b) 1975-1984, and (c) 1995-2004 on one-tenth-degree grid.

The striking feature in Figures 13, 14, and 15 is the repetitiveness of major mesoscale features in climatological annual, seasonal (here in winter as an example in Figure 14), and monthly (here in January as an example in Figure 15) fields. Moreover, the fact that very similar mesoscale patterns (meanders and Gulf Stream eddies) are seen in all decades implies that there is a cumulative effect of mesoscale activities overlaying a clear seasonal signal. The seasonal signal is obviously stronger than the signal generated by mesoscale eddies, but the eddy-type motion is amplified by the seasonal signal. Indeed, repetitive mesoscale patterns superimposed over the seasonal variability must repeat statistically not only every year in each decade, but also every year in all decades since 1955. On the other hand, as the seasonal maps show, there are also distinctive differences between the seasons in the 1955-1964, 1975-1984, and 1995-2004 sequence indicating stochastic nature of mesoscale variability superimposed over the carrying seasonal signal with multi-decadal quasi-periodical cyclicity.

Snapshots of sea surface temperature from both satellite imagery and eddy-resolving numerical simulations (see an example in Figure 4) reveal a strong resemblance to the NWA high-resolution monthly regional climatologies. Importantly, those monthly averaged temperatures show an individual realization of the jet stream and mesoscale eddies and there is no guarantee that averaging over a long time period would yield similar resemblance (years and decades compared to week and months as a characteristic time scale of the mesoscale variability). Nonetheless, there is a line of thinking that mesoscale variability is interlocked with seasonal cyclicity and that there is a great deal of receptiveness of specific patterns surrounding unstable jet currents, especially the Gulf Stream and Gulf Stream Extension (e.g., Kelly *et al.*, 2010).

As discussed above, the resolution of a regional climatology, either in climate reconstructions using data or in climate modeling, is the key for better understanding the role of regional dynamics in such critical areas such as the Gulf Stream, Kuroshio, etc. Moreover, it is becoming clear that long-term climate forecasting is impossible without detailed knowledge of decadal variability (Siqueira and Kirtman, 2016). Even atmosphere-only sensitivity experiments

have demonstrated the impact of increasing horizontal resolution (Minobe *et al.*, 2008) and that seasonal variability of the Gulf Stream has a substantial impact on the troposphere dynamics (Minobe *et al.*, 2008). In their numerical simulations, Minobe *et al.* (2008) clearly showed that an atmospheric general circulation model with about 50 km resolution responds quite noticeably to the observed sharpness of the Gulf Stream front and they showed that the Gulf Stream affects the entire troposphere. In fact, a poorly resolved Gulf Stream presents a structural problem for atmospheric climate models preventing them from capturing observed decadal climate variability in the North Atlantic (Siqueira and Kirtman, 2016). That is, the sharpness, internal dynamics, and cumulative effect of mesoscale eddies and other transients on decadal scale may become critical for the success of decadal climate forecasting. The key to understanding why decadal climatologies are so important is that they emphasize the repetitiveness or statistical periodicity of the major elements of mesoscale processes in the Gulf Stream system.
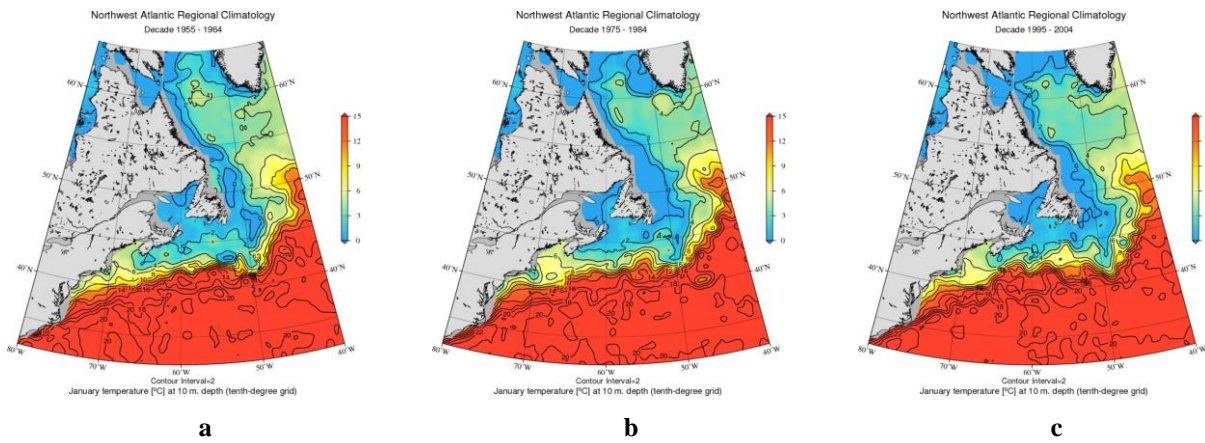

a **b** **c**

Figure 15. January temperature at 10 m depth for three decades: (a) 1955-1964, (b) 1975-1984, and (c) 1995-2004 on one-tenth-degree grid.

Figure 16 reproduces two monthly-averaged satellite sea-surface temperature snapshots, four years apart, in March of 2003 and in 2007, in the Gulf Stream region (Kelly *et al.*, 2010).
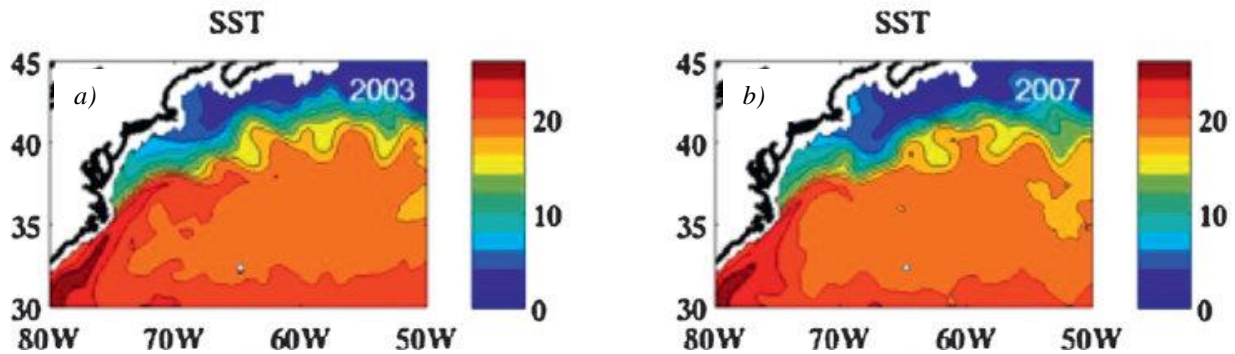
Figure 16. March averages of SST for (a) 2003 and (b) 2007. SST fields are from the Remote Sensing Systems on a 0.258° grid from Kelly *et al.* (2010). ©American Meteorological Society. Used with permission.

As can be seen in Figure 16, although the patterns are not exactly the same (and they would not and should not be expected to repeat exactly, of course), they are surprisingly similar implying the quasi-stationary character of mesoscale variability in the Gulf Stream jet vicinity. In

previous paragraphs, we discussed the striking repetitiveness of the mesoscale temperature patterns, similar to what is shown in Figure 16.

To verify a hypothesis that the seasonal signal carries the superimposed repetitive mesoscale variability, extractions from NWARC were compared with those from eddy-resolving numerical simulations. The model employed for this preliminary data-model comparison is the Nucleus for European Modelling of the Ocean (NEMO) modeling system (Madec, 2008) with a global 1/12th degree grid. The particular simulations that were used here are MJM88 experiments described in detail in Molines *et al.* (2014). These simulations are a part of an extensive international DRAKKAR project using ORCA12 model configuration described, for example, in Molines *et al.* (2014) and Treguier *et al.* (2014). DRAKKAR is a scientific and technical coordination between several European teams. NEMO is a state-of-the-art modeling framework for oceanographic research, operational oceanography seasonal forecast, and climate studies. The output from MJM88 NEMO experiments (courtesy of Jean-Marc Molines of University of Grenoble, France) covers ocean temperature, salinity, velocity and a number of other variables for 55 years, from 1958 to 2012 at 1/12-deg resolution for every 5 days. That is, the computed fields were averaged over each pentad for the entire 55-year interval (Molines *et al.*, 2014).

To compare the simulated and observed climatologies, the model results were averaged over the same decades for which the NWARC were calculated. All model-generated data were averaged for each month of the selected decades. Then seasons were computed as the average of the climatological months, whereas the climatological annual mean was computed as the average of four seasons. The output from the NEMO model was re-plotted in the NWA domain to facilitate easier visual comparison between NWARC and model's results.

Figure 17 shows the temperature at 10m depth averaged over climatological January of 1985-1994 from NWARC (a) and the MJM88 NEMO simulation for the same decade (b), while Figure 18 depicts a similar comparison between NWARC (a) and MJM88 NEMO (b) for July of 1985-1994.

Although we do not expect identical patterns, there are clear similarities between the patterns of observed and modeled climatological months. Moreover, NEMO simulations are on 1/12°x1/12° grid, so some additional inconsistencies because of slight grid resolution differences could be a possibility. Nonetheless, similarities between the maps are quite evident. For example, both climatological Januaries show strong advection along Florida coast with a strong Slope Water Current, while July's temperature shows far warmer water at the Gulf Stream separation point off Cape Hatteras. The series of meanders and eddy-like formations is seen in approximately the same areas and seems to be of similar or at least comparable amplitude. For instance, there is a very pronounced meander of cold water in the MLTZ, in the northeast part of the region in both observed and modelled climatologies. In general, the cumulative impact of mesoscale motion on large-scale circulation dynamics is apparently of the same nature in observed and modelled climatologies.
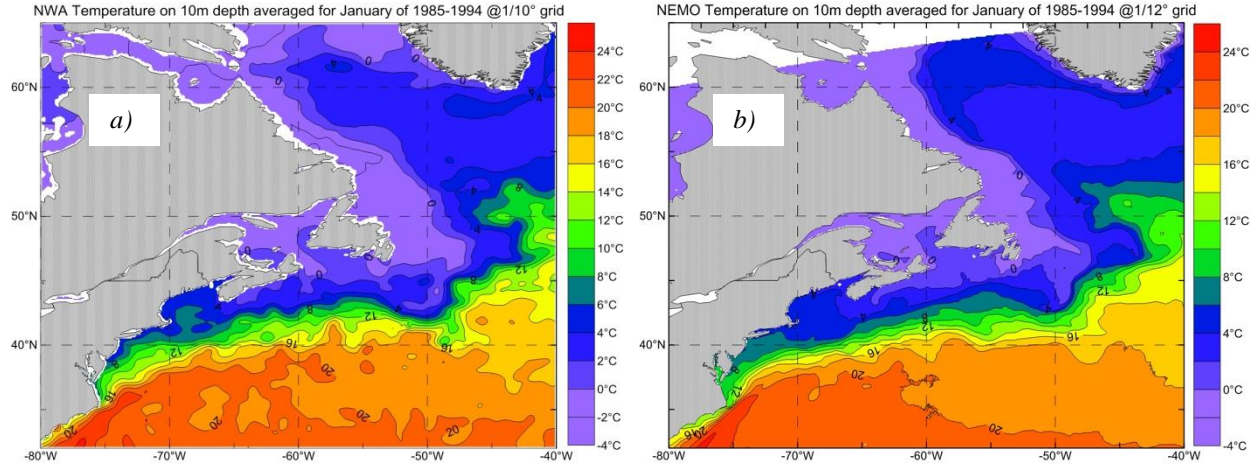
Figure 17. January temperature at 10 m depth from (a) NWARC and (b) the NEMO numerical experiments for the decade 1985-1994.

To support the arguments about similarities between observed and modeled climatologies, Figures 19 and 20 illustrate the differences and the root mean square (RMS) difference, which shows the magnitude of deviations between the observed and modeled decadal temperature at 10 m depth for the decade of 1985-1994. It is clear that in the highly variable zone of unstable jet, RMS difference between observed and model data is higher than in other regions. However, it is surprisingly low almost everywhere else, including the zone of the Gulf Stream core for summer and winter months.
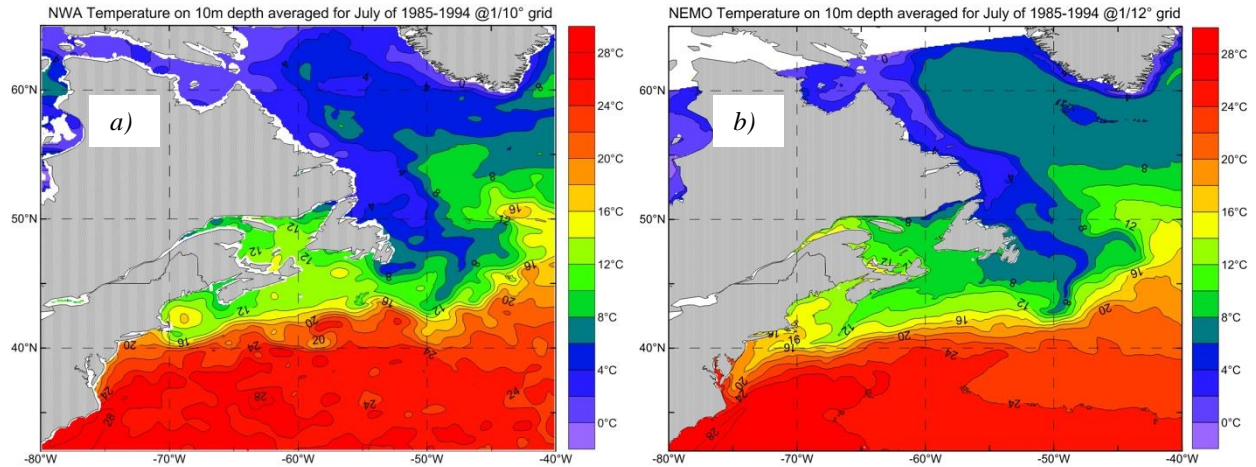

Figure 18. July temperature at 10 m depth from (a) NWARC and (b) the NEMO numerical experiments for the decade 1985-1994.

High-resolution ocean climatologies, like NWARC, may have many uses in climate forecast models, but the most important one may be the use of sea surface salinity (SSS) for restoring in the model spin-up of ocean circulation, which is critical for ocean climate simulations and especially in long-term climate forecasts. As was found in early simulation experiments with coupled ocean-atmosphere models, the freshwater fluxes in such models must be pre-computed using observed SSS to avoid the so-called climate drift, which is an artefact caused by poorly-resolved freshwater fluxes across the ocean surface in practically any coupled ocean-atmosphere model (Bryan, 1998; Huang *et al.*, 2015; Manabe and Stouffer, 1988). After

more than a quarter of a century since such a drift was identified in Manabe and Stouffer (1988), forecast models use the restoring to observed SSS method to suppress such artificial climate drift. Moreover, it has been shown that the SSS from earlier editions of WOA were not sufficient as they are too smooth because of infilling the gaps and objective interpolation on a coarse-resolution grid (e.g., Molines *et al.*, 2014). However, Molines *et al.* (2014) used older one-degree fields. New WOA13, with quarter-degree resolution may already provide sufficiently detailed SSS for such numerical simulations, while for the regions covered by high-resolution climatologies, the best would be using one-tenth-degree grid whenever possible. Providing high-resolution sea surface salinity on quarter- and one-tenth-degree grids with well-resolved frontal structures may be critical for improving long-term ocean climate forecasts.
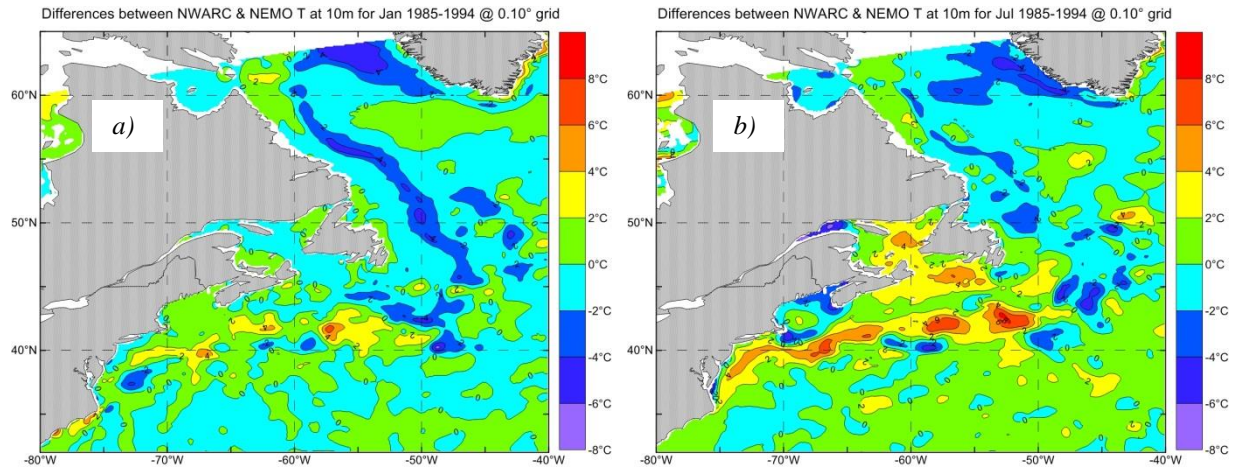

Figure 19. Differences between decadal mean temperature at 10 m depth from NWARC and NEMO model in January (a) and July (b) for the decade of 1985-1994.
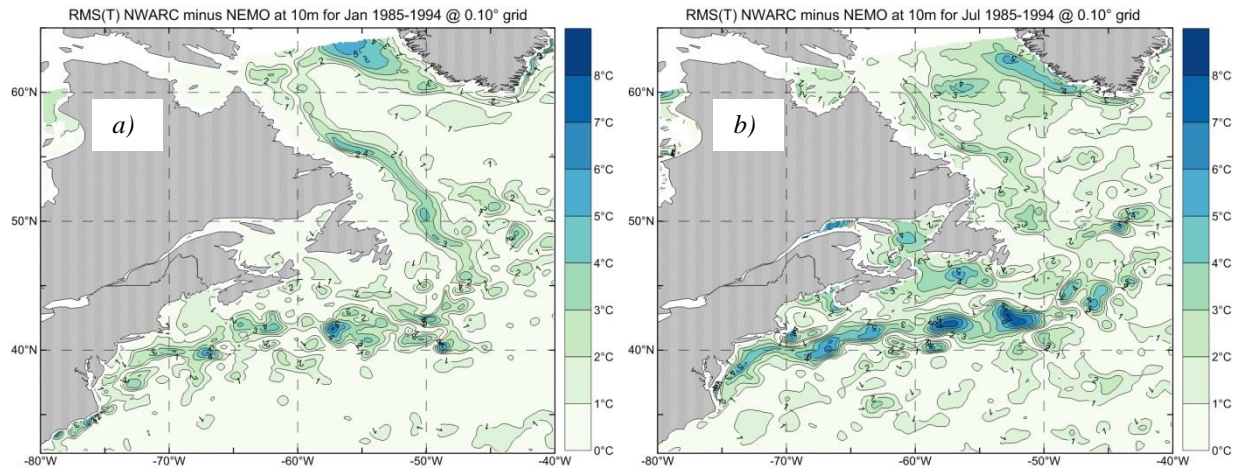

Figure 20. RMS of differences between observed and modeled decadal temperature at 10 m depths in January (a) and July (b) for the decade of 1985-1994 shown on Figure 19.

46

12. SUMMARY

The description and results of the Northwest Atlantic Regional Climatology project aimed at generating objectively analyzed historical ocean temperature and salinity data fields were presented. The effort of creating NWARC resulted in the NWARC Atlas presented in this publication. The advantages of high-resolution regional climatologies along with a discussion of how such climatologies may align with eddy-permitting (or eddy-resolving) ocean numerical modeling were also presented.

Currently, only temperature and salinity decadal climatologies have been created with one-tenth-degree resolution. These climatologies were created to provide investigators in various branches of oceanography, climatology, fisheries, and other related disciplines with oceanographic foundations that define long-term ocean climate change inferred from observations.

When computing anomalies from a standard climatology, it is important that the synoptic field be smoothed to the same extent as the climatology, to prevent generation of spurious anomalies simply through differences in smoothing. However, on finer resolution grids mesoscale eddies are directly resolved and the remaining mesoscale background probably represents a cumulative effect of mesoscale dynamics rather than noise generated by objective analysis. The advantage of a high-resolution grid becomes quite obvious as the shorter radii of influence used in the objective analysis lead to less diffusive fields in the frontal zones with sharp gradients, especially in the coastal regions. In a sense, the finer-resolution analysis suits the same goal as reducing grid sizes in numerical models.

The high-resolution regional climatologies close the gaps between observations and modeling and allow meaningful data-model comparisons in critical regions, such as the Northwest Atlantic Ocean. Moreover, in a new class of long-term ocean climate forecast modeling, the analyzed regional climatologies can be used for restoring the simulated fields to the observed ones (especially sea surface salinity) and thus prevent the climate drift that plagues even the most advanced climate models.

As in all WOA editions and all previous regional climatologies, the goal was to create objectively analyzed fields and data sets that can be used as a "black box" in applications. The new and significant feature we now offer are six high-resolution decadal climatologies that can be used in assessing "true" ocean climate change backed up by aggregated historical oceanographic *in situ* observations. Naturally, some quality control procedures used are somewhat subjective. Moreover, monthly decadal fields are less reliable because of more data gaps than in seasonal or annual fields, so some mesoscale features could still be affected by artefacts caused by lack of data. However, seasonal and annual fields are very well supported by data, especially in decades that are more recent.

Disclaimer: Users of the NWARC, and all other high-resolution regional climatologies for that matter, are advised to inspect very carefully the data distributions, statistical means, standard errors, etc., before deciding to what extent they can rely on our objectively analyzed data and maps in their mission-critical research and application developments. For those users who wish to make their own choices, all data used in WOA13 and NWARC analyses, both at standard and observed depth levels, are available at the WOD13 web site.

In very rare cases, some maps at some depths in monthly fields in the Atlas, especially in earlier decades, may show some peculiarities that may be due to non-representativeness of data and have not yet been flagged by manual quality control described in the text. Although we have made all possible effort to eliminate as many of these features as possible by flagging the data that generate such features, some could still be undetected and remain unflagged. Some may eventually turn out not to be artefacts, but rather represents real features. In such rare cases, we are not capable yet to describe and explain them in any meaningful way due to lack of data. In any of such cases, which are very few, users are advised to be extremely cautious and make all possible efforts to recognize where the analyzed fields are sufficiently supported by observations by using the supplied additional statistical fields, such as simple statistics, number of available observations, standard errors, etc.

13. FUTURE WORK

Our analyses will be updated when justified by newly available observations. As more data are received and archived in WOD, there may be a ground to produce improved higher resolution climatologies for temperature and salinity and perhaps for some other essential oceanographic variables. The NWARC will be updated in concert with the next update of WOA, which will be denoted WOA17, and is expected to be published in 2017. Moreover, other regional climatologies will undergo major revisions by adding seasonal and annual decadal climatologies for the six decades since 1955 with high resolution wherever it may be feasible. The nearest future high-resolution regional climatology is the Northern North Pacific regional climatology, which is currently under development and is expected to be published in 2017 as well.

14. REFERENCES

Allison, E. H., A. L. Perry, M.-C. Badjeck, W. Neil Adger, K. Brown, D. Conway, A. S. Halls, G. M. Pilling, J. D. Reynolds, N. L. Andrew, and N. K. Dulvy (2009), Vulnerability of national economies to the impacts of climate change on fisheries, Fish and Fisheries, 10(2), 173-196, doi:10.1111/j.1467-2979.2008.00310.x.

Antonov, J. I., D. Seidov, T. P. Boyer, R. A. Locarnini, A. V. Mishonov, and H. E. Garcia (2010), World Ocean Atlas 2009, Volume 2: Salinity, in *NOAA Atlas NESDIS*, edited by S. Levitus, p. 184, U.S. Government Printing Office, Washington, D.C.

Arguez, A., and R. S. Vose (2011), The Definition of the Standard WMO Climate Normal: The Key to Deriving Alternative Climate Normals, *Bulletin of the American Meteorological Society*, *92*(6), 699-704, doi:10.1175/2010bams2955.1.

Barange, M., and R. P. Harris (2010), *Marine ecosystems and global change*, Oxford University Press Oxford.

Barnes, S. L. (1964), A Technique for Maximizing Details in Numerical Weather Map Analysis, *Journal of Applied Meteorology*, *3*(4), 396-409, doi:10.1175/1520-0450(1964)003<0396:atfmdi>2.0.co;2.

Barnes, S. L. (1973), Mesoscale objective map analysis using weighted time series observations, in *NOAA Technical Memorandum ERL NSSL 62*, edited, Wash. D.C.

Barnes, S. L. (1994), Applications of the Barnes Objective Analysis Scheme. Part III: Tuning for Minimum Error, *Journal of Atmospheric and Oceanic Technology*, *11*(6), 1459-1479, doi:10.1175/1520-0426(1994)011.

Barrier, N., J. Deshayes, A.-M. Treguier, and C. Cassou (2015), Heat budget in the North Atlantic subpolar gyre: impacts of atmospheric weather regimes on the 1995 warming event, *Progress in Oceanography*(0), 75-90, doi:http://dx.doi.org/10.1016/j.pocean.2014.10.001.

Belkin, I. M., S. Levitus, J. Antonov, and S.-A. Malmberg (1998), "Great Salinity Anomalies" in the North Atlantic, *Progress In Oceanography*, *41*(1), 1-68, doi:10.1016/s0079-6611(98)00015-9.

Bernard, J. L., *and Co-authors* (2006), Impact of partial steps and momentum advection schemes in a global ocean circulation model at eddy-permitting resolution, *Ocean Dynamics*, *56*(5), 543-567, doi:10.1007/s10236-006-0082-1.

Blanchard, J. L., S. Jennings, R. Holmes, J. Harle, G. Merino, J. I. Allen, J. Holt, N. K. Dulvy, and M. Barange (2012), Potential consequences of climate change for primary production and fish production in large marine ecosystems, *Philosophical Transactions of the Royal Society of London B: Biological Sciences*, *367*(1605), 2979-2989, doi:10.1098/rstb.2012.0231.

Blunden, J., and D. S. Arndt (2014), State of the Climate in 2013, Bulletin of the American Meteorological Society, 95(7), S1-S279, doi:10.1175/2014BAMSStateoftheClimate.1.

Blunden, J., and D. S. Arndt (2015), State of the Climate in 2014, *Bulletin of the American Meteorological Society*, 96(7), ES1-ES32, doi:10.1175/2015BAMSStateoftheClimate.1.

Bower, A. S., H. T. Rossby, and J. L. Lillibridge (1985), The Gulf Stream-Barrier or blender?, *Journal of Physical Oceanography*, *15*(1), 24-32.

Boyer, T., S. Levitus, H. Garcia, R. A. Locarnini, C. Stephens, and J. Antonov (2005), Objective analyses of annual, seasonal, and monthly temperature and salinity for the

World Ocean on a 0.25° grid, International Journal of Climatology, 25(7), 931-945, doi:10.1002/joc.1173.

Boyer, T. P., and Co-authors (2013), World Ocean Database 2013, in NOAA Atlas NESDIS 72, edited by S. Levitus, p. 209, U.S. Government Printing Office, Washington, D.C.

Brander, K. (2010), Impacts of climate change on fisheries, Journal of Marine Systems, 79(3–4), 389-402, doi:http://dx.doi.org/10.1016/j.jmarsys.2008.12.015.

Broecker, W. (1991), The great ocean conveyor, Oceanography, 1, 79-89.

Bryan, F. O. (1998), Climate drift in a multicentury integration of the NCAR climate system model, Journal of Climate, 11(6), 1455-1471.

Bryan, K. (1986), Poleward buoyancy transport in the ocean and mesoscale eddies, Journal of Physical Oceanography, 16(5), 927-933.

Bryden, H. L., H. R. Longworth, and S. A. Cunningham (2005), Slowing of the Atlantic meridional overturning circulation at 25°N, Nature, 438(7068), 655-657.

Buckley, M. W., and J. Marshall (2016), Observations, inferences, and mechanisms of Atlantic Meridional Overturning Circulation variability: A review, Reviews of Geophysics, n/a-n/a, doi:10.1002/2015RG000493.

Chao, Y., A. Gangopadhyay, F. O. Bryan, and W. R. Holland (1996), Modeling the Gulf Stream System: How far from reality?, Geophys. Res. Let., 23(22), 3155-3158, doi:10.1029/96GL03003.

Charney, J. G. (1971), Geostrophic Turbulence, Journal of Atmospheric Sciences, 28, 1087-1095, doi:http://dx.doi.org/10.1175/1520-0469(1971).

Chelton, D. B., M. G. Schlax, and R. M. Samelson (2011), Global observations of nonlinear mesoscale eddies, Progress in Oceanography, 91(2), 167-216, doi:http://dx.doi.org/10.1016/j.pocean.2011.01.002.

Climate Change 2014: Synthesis Report. Contribution of Working Groups I, II and III to the Fifth Assessment Report of the Intergovernmental Panel on Climate Change, in IPCC, 2014, edited by P. Core Writing Team, R. K. & Meyer, L. (eds), p. 151, IPCC, Geneva, Switzerland.

Cox, M. (1975), A baroclinic numerical model of the world ocean: Preliminary results, in Numerical Models of Ocean Circulation, edited, pp. 107-120, National Academy of Sciences, Washington, DC.

Cunningham, S. A., T. Kanzow, D. Rayner, M. O. Baringer, W. E. Johns, J. Marotzke, H. R. Longworth, E. M. Grant, J. J. M. Hirschi, L. M. Beal, C. S. Meinen, and H. L. Bryden (2007), Temporal Variability of the Atlantic Meridional Overturning Circulation at 26.5°N, Science, 317(5840), 935-938, doi:10.1126/science.1141304.

Delworth, T. L., R. Zhang, and M. E. Mann (2007), Decadal to centennial variability of the Atlantic from observations and models, in Ocean Circulation: Mechanisms and Impacts – Past and Future Changes of Meridional Overturning, edited, pp. 131-148, AGU, Washington, DC, doi:10.1029/173gm10.

Drinkwater, K. F. (2005), The response of Atlantic cod (Gadus morhua) to future climate change, ICES J. Mar. Sci., 62(7), 1327-1337, doi:10.1016/j.icesjms.2005.05.015.

Drinkwater, K. F., F. Mueter, K. D. Friedland, M. Taylor, G. L. Hunt Jr, J. Hare, and W. Melle (2009), Recent climate forcing and physical oceanographic changes in Northern Hemisphere regions: A review and comparison of four marine ecosystems, *Progress In Oceanography*, *81*(1–4), 10-28, doi:10.1016/j.pocean.2009.04.003.

Drinkwater, K. F., M. Miles, I. Medhaug, O. H. Otterå, T. Kristiansen, S. Sundby, and Y. Gao (2013), The Atlantic Multidecadal Oscillation: Its manifestations and impacts with special emphasis on the Atlantic region north of 60°N, Journal of Marine Systems(0), doi:http://dx.doi.org/10.1016/j.jmarsys.2013.11.001.

Frajka-Williams, E., P. B. Rhines, and C. C. Eriksen (2009), Physical controls and mesoscale variability in the Labrador Sea spring phytoplankton bloom observed by Seaglider, Deep Sea Research Part I: Oceanographic Research Papers, 56(12), 2144-2161, doi:http://dx.doi.org/10.1016/j.dsr.2009.07.008.

Frankignoul, C., G. de Coëtlogon, T. M. Joyce, and S. Dong (2001), Gulf Stream Variability and Ocean–Atmosphere Interactions*, Journal of Physical Oceanography, 31(12), 3516-3529, doi:10.1175/1520-0485(2002)031<3516:GSVAOA>2.0.CO;2.

Fuglister, F. C. (1963), Gulf Stream - 60, Progress In Oceanography, 1, 265-272.

Goosse, H., and M. M. Holland (2005), Mechanisms of Decadal Arctic Climate Variability in the Community Climate System Model, Version 2 (CCSM2), Journal of Climate, 18(17), 3552-3570.

Gordon, A. L. (1986), Interocean exchange of thermocline water, Journal of Geophysical Research, 91, 5037-5046.

Gould, J., and Co-authors (2004), Argo profiling floats bring new era of in situ ocean observations, Eos, Transactions American Geophysical Union, 85(19), 185-191, doi:10.1029/2004EO190002.

Gula, J., M. J. Molemaker, and J. C. McWilliams (2016), Submesoscale Dynamics of a Gulf Stream Frontal Eddy in the South Atlantic Bight, Journal of Physical Oceanography, 46(1), 305-325, doi:10.1175/JPO-D-14-0258.1.

Guttman, N. B. (1989), Statistical Descriptors of Climate, Bulletin of the American Meteorological Society, 70(6), 602-607, doi:10.1175/1520-0477(1989)070<0602:SDOC>2.0.CO;2.

Hogg, N. G., R. S. Pickart, R. M. Hendry, and W. J. Smethie Jr (1986), The northern recirculation gyre of the gulf Stream, Deep Sea Research Part A. Oceanographic Research Papers, 33(9), 1139-1165, doi:http://dx.doi.org/10.1016/0198-0149(86)90017-8.

Hogg, N. G., and W. E. Johns (1995), Western boundary currents, Reviews of Geophysics, 33(S2), 1311-1334, doi:10.1029/95RG00491.

Holt, J., J. Harle, R. Proctor, S. Michel, M. Ashworth, C. Batstone, I. Allen, R. Holmes, T. Smyth, K. Haines, D. Bretherton, and G. Smith (2009), Modelling the global coastal ocean, Philosophical Transactions of the Royal Society of London A: Mathematical, Physical and Engineering Sciences, 367(1890), 939-951, doi:10.1098/rsta.2008.0210.

Holt, J., and Co-authors (2014), Challenges in integrative approaches to modelling the marine ecosystems of the North Atlantic: Physics to fish and coasts to ocean, Progress in Oceanography, 129, Part B(0), 285-313, doi:http://dx.doi.org/10.1016/j.pocean.2014.04.024.

Hu, A., and G. A. Meehl (2005), Bering Strait throughflow and the thermohaline circulation, Geophys. Res. Lett., 32(24), L24610, doi:24610.21029/22005GL024424, doi:10.1029/2005gl024424.

Huang, B., J. Zhu, L. Marx, X. Wu, A. Kumar, Z.-Z. Hu, M. A. Balmaseda, S. Zhang, J. Lu, E. K. Schneider, and J. L. Kinter III (2015), Climate drift of AMOC, North Atlantic

salinity and arctic sea ice in CFSv2 decadal predictions, Climate Dynamics, 44(1), 559-583, doi:10.1007/s00382-014-2395-y.

Isachsen, P. E., S. R. Sørlie, C. Mauritzen, C. Lydersen, P. Dodd, and K. M. Kovacs (2014), Upper-ocean hydrography of the Nordic Seas during the International Polar Year (2007–2008) as observed by instrumented seals and Argo floats, Deep Sea Research Part I: Oceanographic Research Papers, 93(0), 41-59, doi:http://dx.doi.org/10.1016/j.dsr.2014.06.012.

Iselin, C. (1936), A study of the circulation of the western North Atlantic, in Papers in Physical Oceanography and Meteorology, edited, p. 101.

Iselin, C. O. D., and F. C. Fuglister (1948), Some recent developments in the study of the Gulf Stream, J. Mar. Res., 7, 317-329.

Jackett, D. R., and T. J. McDougall (1995), Minimal Adjustment of Hydrographic Profiles to Achieve Static Stability, Journal of Atmospheric and Oceanic Technology, 12(2), 381-389, doi:10.1175/1520-0426(1995)012<0381:MAOHPT>2.0.CO;2.

Jennings, S., and K. Brander (2010), Predicting the effects of climate change on marine communities and the consequences for fisheries, Journal of Marine Systems, 79(3–4), 418-426, doi:http://dx.doi.org/10.1016/j.jmarsys.2008.12.016.

Johnson, D. R., T. P. Boyer, H. E. Garcia, R. A. Locarnini, O. K. Baranova, and M. M. Zweng (2013), World Ocean Database 2013 User's Manual: NODC Internal Report, edited, p. 172, U.S. Government Printing Office, Washington, D.C.

Joyce, T. M., L. N. Thomas, W. K. Dewar, and J. B. Girton (2013), Eighteen Degree Water formation within the Gulf Stream during CLIMODE, Deep Sea Research Part II: Topical Studies in Oceanography, 91, 1-10, doi:http://dx.doi.org/10.1016/j.dsr2.2013.02.019.

Kamenkovich, V. M., M. N. Koshlyakov, and A. S. Monin (1986), Synoptic eddies in the ocean, 433 pp., Reidel, Dordrecht, holland.

Kamykowski, D. (2014), Twentieth century Atlantic meridional overturning circulation as an indicator of global ocean multidecadal variability: influences on sea level anomalies and small pelagic fishery synchronies, ICES Journal of Marine Science: Journal du Conseil, 71(3), 455-468, doi:10.1093/icesjms/fst165.

Kelly, K. A., R. J. Small, R. M. Samelson, B. Qiu, T. M. Joyce, Y.-O. Kwon, and M. F. Cronin (2010), Western Boundary Currents and Frontal Air–Sea Interaction: Gulf Stream and Kuroshio Extension, Journal of Climate, 23(21), 5644-5667, doi:10.1175/2010JCLI3346.1.

Klatt, O., O. Boebel, and E. Fahrbach (2007), A Profiling Float's Sense of Ice, Journal of Atmospheric and Oceanic Technology, 24(7), 1301-1308, doi:10.1175/JTECH2026.1.

Klymak, J. M., R. K. Shearman, J. Gula, C. M. Lee, E. A. D'Asaro, L. N. Thomas, R. R. Harcourt, A. Y. Shcherbina, M. A. Sundermeyer, J. Molemaker, and J. C. McWilliams ((2016), Submesoscale streamers exchange water on the north wall of the Gulf Stream, Geophys. Res. Let., 43(3), 1226-1233, doi:10.1002/2015GL067152.

Lehodey, P., and Co-authors (2006), Climate Variability, Fish, and Fisheries, Journal of Climate, 19(20), 5009-5030.

Leterme, S. C., and R. D. Pingree (2008), The Gulf Stream, rings and North Atlantic eddy structures from remote sensing (Altimeter and SeaWiFS), Journal of Marine Systems, 69(3–4), 177-190, doi:http://dx.doi.org/10.1016/j.jmarsys.2005.11.022.

Levitus, S. (1982), Climatological Atlas of the World Ocean, 190 pp., Rockville, MD.

Levitus, S., J. I. Antonov, T. P. Boyer, and C. Stephens (2000), Warming of the World Ocean, Science, 287, 2225-2229.

Levitus, S., J. I. Antonov, T. P. Boyer, R. A. Locarnini, H. E. Garcia, and A. V. Mishonov (2009), Global ocean heat content 1955-2008 in light of recently revealed instrumentation problems, Geophys. Res. Lett., 36, L07608, doi:07610.01029/02008GL037155.

Levitus, S., J. I. Antonov, T. P. Boyer, O. K. Baranova, H. E. Garcia, R. A. Locarnini, A. V. Mishonov, J. R. Reagan, D. Seidov, E. S. Yarosh, and M. M. Zweng (2012), World ocean heat content and thermosteric sea level change (0–2000 m), 1955–2010, Geophys. Res. Lett., 39(10), L10603, doi:10610.11029/12012GL051106, doi:10.1029/2012gl051106.

Livezey, R. E., K. Y. Vinnikov, M. M. Timofeyeva, R. Tinker, and H. M. v. d. Dool (2007), Estimation and Extrapolation of Climate Normals and Climatic Trends, Journal of Applied Meteorology and Climatology, 46(11), 1759-1776, doi:10.1175/2007JAMC1666.1.

Locarnini, R. A., A. V. Mishonov, J. I. Antonov, T. P. Boyer, and H. E. Garcia (2010), World Ocean Atlas 2009, Volume 1: Temperature., in NOAA Atlas NESDIS, edited by S. Levitus, p. 184, U.S. Government Printing Office, Washington, D.C.

Locarnini, R. A., A. V. Mishonov, J. I. Antonov, T. P. Boyer, H. E. Garcia, O. K. Baranova, M. M. Zweng, C. R. Paver, J. R. Reagan, D. R. Johnson, M. Hamilton, and D. Seidov (2013), World Ocean Atlas 2013, Volume 1: Temperature, in NOAA Atlas NESDIS, edited by S. Levitus, p. 40 pp, NOAA/NESDIS, Washington, D.C.

Lynn, R. J., and J. L. Reid (1968), Characteristics and circulation of deep and abyssal waters, Deep Sea Research and Oceanographic Abstracts, 15(5), 577-598, doi:http://dx.doi.org/10.1016/0011-7471(68)90064-8.

Madec, G. (2008), NEMO ocean general circulation model reference manual, in Internal Report, edited, LODYC/IPSL Paris.

Maltrud, M. E., and J. L. McClean (2005), An eddy resolving global 1/10° ocean simulation, Ocean Modelling, 8(1-2), 31-54.

Manabe, S., and R. J. Stouffer (1988), Two stable equilibria of a coupled ocean-atmosphere model, Journal of Climate, 1, 841-866.

Mann, K. H., and J. R. Lazier (2013), Dynamics of marine ecosystems: biological-physical interactions in the oceans, John Wiley & Sons.

Marshall, J., and G. Nurser (1988), On the recirculation of the subtropical gyre, Quarterly Journal of the Royal Meteorological Society, 114(484), 1517-1534, doi:10.1002/qj.49711448408.

Marzocchi, A., J. J. M. Hirschi, N. P. Holliday, S. A. Cunningham, A. T. Blaker, and A. C. Coward (2015), The North Atlantic subpolar circulation in an eddy-resolving global ocean model, Journal of Marine Systems, 142, 126-143, doi:http://dx.doi.org/10.1016/j.jmarsys.2014.10.007.

McCarthy, G. D., D. A. Smeed, W. E. Johns, E. Frajka-Williams, B. I. Moat, D. Rayner, M. O. Baringer, C. S. Meinen, J. Collins, and H. L. Bryden (2015), Measuring the Atlantic Meridional Overturning Circulation at 26°N, Progress in Oceanography(0), 91-111, doi:http://dx.doi.org/10.1016/j.pocean.2014.10.006.

Minobe, S., A. Kuwano-Yoshida, N. Komori, S.-P. Xie, and R. J. Small (2008), Influence of the Gulf Stream on the troposphere, Nature, 452(7184), 206-209, doi:http://www.nature.com/nature/journal/v452/n7184/suppinfo/nature06690_S1.html.

Molines, J., B. Barnier, T. Penduff, A. Treguier, and J. Le Sommer (2014), ORCA12. L46 climatological and interannual simulations forced with DFS4.4: GJM02 and MJM88. Drakkar Group Experiment Report GDRI-DRAKKAR-2014-03-19, 50 pp. (Available online at http://www.drakkar-ocean.eu/publications/reports/orca12_reference_—experiments_2014).

Monin, A. S. (1986), An introduction into the theory of climate, 261 pp., D. Reidel Publishing Company, Dordrecht.

Munk, W. H. (1950), On the wind-driven ocean circulation, Journal of Meteorology, 7(2), 79-93.

Nakamura, M., and T. Kagimoto (2006), Transient wave activity and its fluxes in the North Atlantic Ocean simulated by a global eddy-resolving model, Dyn.Atmos.Oceans, 41(1), 60-84.

Nye, J. A., M. R. Baker, R. Bell, A. Kenny, K. H. Kilbourne, K. D. Friedland, E. Martino, M. M. Stachura, K. S. Van Houtan, and R. Wood (2014), Ecosystem effects of the Atlantic Multidecadal Oscillation, Journal of Marine Systems, 133(0), 103-116, doi:http://dx.doi.org/10.1016/j.jmarsys.2013.02.006.

Overland, J. E., J. Alheit, A. Bakun, J. W. Hurrell, D. L. Mackas, and A. J. Miller (2010), Climate controls on marine ecosystems and fish populations, Journal of Marine Systems, 79(3–4), 305-315, doi:http://dx.doi.org/10.1016/j.jmarsys.2008.12.009.

Rayner, D., J. J. M. Hirschi, T. Kanzow, W. E. Johns, P. G. Wright, E. Frajka-Williams, H. L. Bryden, C. S. Meinen, M. O. Baringer, J. Marotzke, L. M. Beal, and S. A. Cunningham (2011), Monitoring the Atlantic meridional overturning circulation, Deep Sea Research Part II: Topical Studies in Oceanography, 58(17–18), 1744-1753, doi:http://dx.doi.org/10.1016/j.dsr2.2010.10.056.

Rhines, P. B. (1979), Geostrophic Turbulence, Annual Review of Fluid Mechanics, 11, 401-441, doi:10.1146/annurev.fl.11.010179.002153.

Rhines, P. B. (2001), Mesoscale eddies: Encyclopedia of ocean sciences, edited, pp. 1717-1730, Elsevier Science Ltd, London.

Richardson, P. L. (1983), Eddy kinetic energy in the North Atlantic from surface drifters, Journal of Geophysical Research: Oceans, 88(C7), 4355-4367, doi:10.1029/JC088iC07p04355.

Richardson, P. L. (2001), Florida Current, Gulf Stream and Labrador Current Steele, John H, in Encyclopedia of Ocean Sciences, edited by J.H. Steele, pp. 1054-1064, Academic Press, Oxford, doi:http://dx.doi.org/10.1006/rwos.2001.0357.

Riser, S. C., and Co-authors (2016), Fifteen years of ocean observations with the global Argo array, Nature Clim. Change, 6(2), 145-153, doi:10.1038/nclimate2872.

Roemmich, D., and W. B. Owens (2002), The ARGO project: Global ocean observations for understanding and prediction of climate variability, Oceanography, 13(2), 45– 50.

Roemmich, D., G. C. Johnson, S. Riser, R. Davis, J. Gilson, W. B. Owens, S. L. Garzoli, C. Schmid, and M. Ignaszewski (2009), The Argo Program: Observing the global ocean with profiling floats, Oceanography, 22(2), 34-43, doi:http://dx.doi.org/10.5670/oceanog.2009.36#sthash.fUVBu2wX.dpuf.

Rossby, T., C. Flagg, and K. Donohue (2010), On the variability of Gulf Stream transport from seasonal to decadal timescales, Journal of Marine Research, 68(3-1), 503-522, doi:10.1357/002224010794657128.

Rossby, T., C. N. Flagg, K. Donohue, A. Sanchez-Franks, and J. Lillibridge (2014), On the long-term stability of Gulf Stream transport based on 20 years of direct measurements, Geophys. Res. Let., 41(1), 2013GL058636, doi:10.1002/2013GL058636.

Sarmiento, J. L., and Co-authors (2004), Response of ocean ecosystems to climate warming, Global Biogeochemical Cycles, 18(GB3003), 23.

Schmittner, A. (2005), Decline of the marine ecosystem caused by a reduction in the Atlantic overturning circulation, Nature, 434, 628-633.

Schmitz, W. J., Jr., and M. S. McCartney (1993), On the North Atlantic circulation, Reviews of Geophysics, 31, 29-49.

Schollaert, S. E., T. Rossby, and J. A. Yoder (2004), Gulf Stream cross-frontal exchange: possible mechanisms to explain interannual variations in phytoplankton chlorophyll in the Slope Sea during the SeaWiFS years, Deep Sea Research Part II: Topical Studies in Oceanography, 51(1–3), 173-188, doi:http://dx.doi.org/10.1016/j.dsr2.2003.07.017.

Seidov, D. (1989), Synergetics of the ocean circulation, in Mesoscale/synoptic coherent structures in geophysical turbulence, edited by J. C. J. Nihoul and B. M. Jamart, 797-819, Elsevier, Amsterdam.

Seidov, D., J. I. Antonov, K. M. Arzayus, O. K. Baranova, M. Biddle, T. P. Boyer, D. R. Johnson, A. V. Mishonov, C. Paver, and M. M. Zweng (2015), Oceanography north of 60°N from World Ocean Database, Progress in Oceanography, 132, 153-173, doi:http://dx.doi.org/10.1016/j.pocean.2014.02.003.

Seidov, D. G., and A. D. Maruskevich (1992), Order and chaos in ocean current dynamics:numerical experiment, Dyn.Atmos.Oceans, 16, 405-434.

Semtner, A. J., and R. M. Chervin (1988), A simulation of the global ocean circultion with resolved eddies, Journal of Geophysical Research, 93, 15502-15522.

Semtner, A. J., and R. M. Chervin (1993), Including eddies in global ocean models, Eos, Trans., Amer. Geophys. Union, 74, 59.

Semtner, A. J. (1995), Modeling Ocean Circulation, Science, 269(5229), 1379-1385, doi:10.1126/science.269.5229.1379.

Shackell, N. L., A. Bundy, J. A. Nye, and J. S. Link (2012), Common large-scale responses to climate and fishing across Northwest Atlantic ecosystems, ICES Journal of Marine Science: Journal du Conseil, doi:10.1093/icesjms/fsr195.

Sherman, K., I. Belkin, K. D. Friedland, and J. O'Reilly (2013), Changing states of North Atlantic large marine ecosystems, Environmental Development, 7(0), 46-58, doi:http://dx.doi.org/10.1016/j.envdev.2013.05.004.

Siqueira, L., and B. P. Kirtman (2016), Atlantic near-term climate variability and the role of a resolved Gulf Stream, Geophys. Res. Let., 43(8), 3964-3972, doi:10.1002/2016GL068694.

Skjoldal, H. R., and K. Sherman (2002), Large marine ecosystems of the North Atlantic: changing states and sustainability, Elsevier.

Smeed, D. A., G. McCarthy, S. A. Cunningham, E. Frajka-Williams, D. Rayner, W. E. Johns, C. S. Meinen, M. O. Baringer, B. I. Moat, A. Duchez, and H. L. Bryden (2014), Observed decline of the Atlantic Meridional Overturning Circulation 2004 to 2012, Ocean Sci. , 10(5), 29-38, doi:10.5194/os-10-29-2014.

Srokosz, M., M. Baringer, H. Bryden, S. Cunningham, T. Delworth, S. Lozier, J. Marotzke, and R. Sutton (2012), Past, Present, and Future Changes in the Atlantic Meridional

Overturning Circulation, Bulletin of the American Meteorological Society, 93(11), 1663-1676, doi:10.1175/bams-d-11-00151.1.

Stenseth, N. (2004), Marine Ecosystems and Climate Variation: The North Atlantic. A Comparative Perspective, OUP Oxford.

Stommel, H. (1948), The westward intensification of the wind-driven ocean circulation, Trans. Amer. Geophys. Union, 29, 202-230.

Stommel, H. (1958), The Gulf Stream, 202 pp., University of California, Berkeley, California.

Taylor, A. H. (1996), North–south shifts of the Gulf Stream: Ocean-atmosphere interactions in the North Atlantic, International Journal of Climatology, 16(5), 559-583, doi:10.1002/(SICI)1097-0088(199605)16:5<559::AID-JOC26>3.0.CO;2-Z.

Taylor, J. R. (1997), An Introduction to Error Analysis, 2 ed., University Science Books, Sausalito, CA.

Thomson, R. E., and W. J. Emery (2014), Data analysis methods in physical oceanography, 3d Edition, Third Edition ed., 716 pp., Elsevier, Amsterdam, The Netherlands.

Toole, J. M., R. A. Krishfield, M.-L. Timmermans, and A. Proshutinsky (2011), The Ice-Tethered Profiler: Argo of the Arctic, Oceanography, 24(3), 126-135, doi:http://dx.doi.org/10.5670/oceanog.2011.64.

Treguier, A. M., and Co-authors (2014), Meridional transport of salt in the global ocean from an eddy-resolving model, Ocean Sci., 10(2), 243-255, doi:10.5194/os-10-243-2014.

Wessel, P. and W. H. F. Smith, New, improved version of the Generic Mapping Tools released, EOS Trans. AGU, 79, 579, 1998.

WMO (2011), World Metoroilogical Organization: Guide to Climatological Practices, 2011 Edition ed., WMO, Geneva, Switzerland.

Wong, A. P. S., and S. C. Riser (2011), Profiling Float Observations of the Upper Ocean under Sea Ice off the Wilkes Land Coast of Antarctica, Journal of Physical Oceanography, 41(6), 1102-1115, doi:10.1175/2011JPO4516.1.

Wong, A. P. S., and S. C. Riser (2013), Modified shelf water on the continental slope north of Mac Robertson Land, East Antarctica, Geophys. Res. Let., 40(23), 6186-6190, doi:10.1002/2013GL058125.

Worthington, L. V. (1976), On the North Atlantic circulation, 110 pp., Johns Hopkins University Press.

Wunsch, C. (1978), The North Atlantic general circulation west of 50°W determined by inverse methods, Reviews of Geophysics, 16(4), 583-620, doi:10.1029/RG016i004p00583.

Yashayaev, I., D. Seidov, and E. Demirov (2015), A new collective view of oceanography of the Arctic and North Atlantic basins, Progress in Oceanography, 132(0), 1-21, doi:http://dx.doi.org/10.1016/j.pocean.2014.12.012.

Zweng, M. M., J. R. Reagan, J. I. Antonov, R. A. Locarnini, A. V. Mishonov, T. P. Boyer, H. E. Garcia, O. K. Baranova, D. R. Johnson, D. Seidov, and M. M. Biddle (2013), World Ocean Atlas 2013, Volume 2: Salinity, in NOAA Atlas NESDIS, edited by S. Levitus, p. 39, NOAA/NESDIS, Washington, D.C.